

# ChemComm

Accepted Manuscript



This article can be cited before page numbers have been issued, to do this please use: E. Spuling, N. Sharma, I. Samuel, E. Zysman-Colman and S. Braese, *Chem. Commun.*, 2018, DOI: 10.1039/C8CC04594A.



This is an Accepted Manuscript, which has been through the Royal Society of Chemistry peer review process and has been accepted for publication.

Accepted Manuscripts are published online shortly after acceptance, before technical editing, formatting and proof reading. Using this free service, authors can make their results available to the community, in citable form, before we publish the edited article. We will replace this Accepted Manuscript with the edited and formatted Advance Article as soon as it is available.

You can find more information about Accepted Manuscripts in the [author guidelines](#).

Please note that technical editing may introduce minor changes to the text and/or graphics, which may alter content. The journal's standard [Terms & Conditions](#) and the ethical guidelines, outlined in our [author and reviewer resource centre](#), still apply. In no event shall the Royal Society of Chemistry be held responsible for any errors or omissions in this Accepted Manuscript or any consequences arising from the use of any information it contains.

# Chemical Communications

## Guidelines for referees

View Article Online  
DOI: 10.1039/C8CC04594A



*ChemComm* is a forum for urgent high quality communications from across the chemical sciences.

Communications in *ChemComm* should be preliminary accounts of **original and urgent work** of significance to a general chemistry audience. The 2016 impact factor for *ChemComm* is **6.319**.

Only work within the top 25% of the field in terms of quality and interest should be recommended for publication. Acceptance should only be recommended if the content is of such **urgency and significant general interest** that rapid publication will be advantageous to the progress of chemical research.

**Routine and incremental work – however competently researched and reported – should not be recommended for publication.**

**Articles which rely excessively on supplementary information should not be recommended for publication.**

Thank you very much for your assistance in evaluating this manuscript.

### General Guidance

Referees have the responsibility to treat the manuscript as confidential. Please be aware of our [Ethical Guidelines](#), which contain full information on the responsibilities of referees and authors, and our [Refereeing Procedure and Policy](#).

#### Supporting information and characterisation of new compounds

Experimental information must be provided to enable other researchers to reproduce the work accurately. It is the responsibility of authors to provide fully convincing evidence for the homogeneity, purity and identity of all compounds they claim as new. This evidence is required to establish that the properties and constants reported are those of the compound with the new structure claimed.

Please assess the evidence presented in support of the claims made by the authors and comment on whether adequate supporting information has been provided to address the above. Further details on the requirements for characterisation criteria can be found [here](#).

#### When preparing your report, please:

- comment on the originality, significance, impact and scientific reliability of the work;
- state clearly whether you would like to see the article accepted or rejected and give detailed comments (with references, as appropriate) that will both help the Editor to make a decision on the article and the authors to improve it;
- it is the expectation that only work with two strong endorsements will be accepted for publication.

#### Please inform the Editor if:

- there is a conflict of interest;
- there is a significant part of the work which you are not able to referee with confidence;
- the work, or a significant part of the work, has previously been published;
- you believe the work, or a significant part of the work, is currently submitted elsewhere;
- the work represents part of an unduly fragmented investigation.

Submit your report at <http://mc.manuscriptcentral.com/chemcomm>

University  
of  
St Andrews**ELI ZYSMAN-COLMAN, Ph.D., FRSC**School of Chemistry, University of St Andrews,  
Purdie Building, North Haugh  
KY16 9ST[eli.zysman-colman@st-andrews.ac.uk](mailto:eli.zysman-colman@st-andrews.ac.uk)

Tel.: +44-1334 463826; Fax.: +44-1334 463808

<http://www.zysman-colman.com>

01/07/2018

Dear Referees,

We are delighted to hear of the positive assessment of our manuscript. We hope that with these responses and modifications to the manuscript that it now is now in a state to accepted for publication. Below is a point-by-point description of the changes made to the manuscript in response to the points brought up by the referees.

REVIEWER

REPORT(S):

Referee:

1

1. The photoluminescence quantum efficiencies of 3 and 7 in the PMMA and mCP doped film were much lower than those in toluene solutions. In typical cases of TADF emitters, doped films show higher quantum efficiencies than solution state because the molecular motions can be effectively suppressed in the solid phases. The observations in this paper seem to be an opposite. The reviewer expects another intermolecular exciton-quenching process might be occur in the condensed states. The authors should calculate the rate constants for radiative and nonradiative decays, ISC, and RISC for 3 and 7, compare the values between the solution and doped films, and also expand the discussion on this point. This will be of highly importance to further enhance the photoluminescence properties in the solid thin films.

*Many thanks to the referee for highlighting this point.*

*To address this issue, we considered different possibilities that could cause a decrease in PLQY in the solid-state.*

- 1. We considered if aggregation caused quenching is responsible for this behaviour. We measured the PLQY of the mCP thin films at 1 and 3 wt.% doping concentration of 3 and 7. We observed a further decrease in the PLQY at low doping concentration. Increasing the doping concentration beyond 15 wt.% also resulted in a decrease in PLQY (see Table S1).*
- 2. We next examined different host matrices to evaluate the effect of environment and polarity on the PLQY. Regardless of the host used, PLQY remained low, with mCP providing the highest PLQY, regardless of doping concentrations (Table S1).*
- 3. We note that the PLQYs are low and not significantly different for both isomers. Therefore, intramolecular interactions leading to a non-radiative pathway can be ruled out.*
- 4. We analyzed the time-resolved PL spectra of 3 and 7 in PhMe more closely, and the lack of a delayed component in the time-resolved PL spectra in solution would argue that the compounds are not or are only weakly TADF in solution.*

*We therefore have a situation where the compounds are only TADF in the thin film state. The additional nr decay can due to intersystem crossing to the triplet and this loss channel also explains the apparently lower radiative rate decay constant in thin film due to the difference in mechanism of the radiative decay (TADF vs fluorescence).*

*We have calculated the rate constants and added the data to Table S2, page S22. We have assumed that the non-radiative decay rate from S1 is 0 (see justification on page S22). The radiative decay rates in solution are an order of magnitude larger than in the film. This is a function of the different emission mechanisms in the two environments: fluorescence versus TADF.*

2. Related to the comment 1, in the solid state, not only intramolecular exciplex but also intermolecular species can be involved in the TADF process. So, the authors should measure and compare the photophysical properties for the mixture of corresponding benzophenone and triphenylamine derivative (without cyclophane linker) particularly in the doped films. Are there any differences between the mix system and the present cyclophane-linked system?

*We have considered intermolecular interactions (excimer or exciplex between donor and acceptors) by investigating the photophysical behaviour at low doping concentrations. We measured the PLQYs of 3 and 7 at both 1-3 wt.% concentrations in different host matrices (Table S1). We observed a further small decrease in PLQY upon decreasing the doping concentration, regardless of host matrix. These new measurements would suggest that no intermolecular interactions are involved in the TADF process of 3 and 7 or contribute to the decreased PLQY.*

3. Have the authors try to fabricate doped films with much lower concentration of 3 and 7? The reviewer expects higher PL quantum efficiencies in such low-concentration doped film.

*We have followed the referee's helpful suggestion. We measured the PLQYs of 3 and 7 at much lower doping concentrations (1-3 wt.%) in different host matrices (Table S1). Please see our responses to points 1 and 2.*

4. The authors have prepared doped films via vacuum deposition. The prototype OLEDs can thus be constructed by using the same protocol. The authors should provide the data for OLEDs in the revised manuscript. This is very informative for those working in this field.

*The key point of the manuscript is the paradigm shift in design of TADF emitters with the use of paracyclophane as a bridge. These are a new class of materials where coupling between donor and acceptor is mediated through the PCP core. However, PLQYs of both the isomers remained low in their vacuum-deposited films. Therefore, isomers 3 and 7 are not suitable candidates for OLED fabrication. Indeed, with a careful modification in the design, PLQY of such type of emitters can be improved. This is discussed at the end of the paper where we write "We are presently investigating modified designs to mitigate this issue such that paracyclophane-based TADF emitters can be incorporated into OLED devices."*

Referee:

2

1. Upon changing the donor group to the weaker carbazole unit, relatively large  $\Delta E_{ST}$ s were obtained for isomers 4 and 8 in theoretical simulation. It is strongly recommended that the authors carry out more experimental studies to verify the accuracy of DFT calculation.

*We wish to note that we have used a well-established DFT/TDA protocol to calculate the ground and excited state properties of these compounds (J. Chem. Theory Comput. 2015, 11, 168; Phy. Rev. Materials., 2017, 1, 075602). Not unexpectedly,  $\Delta E_{ST}$  increases with decreasing donor strength and the predicted  $S_1$  energy increases. In PhMe we observed a blue-shifted emission at ca. 380 nm for both 4 and 8, which was very very weak. This meant that we could not measure  $\Delta E_{ST}$ . Given the UV nature of the emission, the effective very low PLQY of the emission and the large calculated  $\Delta E_{ST}$  we opted to concentrate our photophysical analyses on promising isomers 3 and 7 exclusively and discounted isomers 4 and 8 as emissive materials for TADF.*

2. The authors presented two isomeric TADF emitters with cis- or trans-structure. However, the authors provided limited comparison of their optoelectronic properties. It is strongly recommended that the authors provide more discussion on the relationship between molecular structures and optoelectronic properties of these two emitters.

*We have added the following text to the manuscript (page 3)*

*“The optoelectronic properties of 3 and 7 are influenced by the relative configuration of D and A. A red-shift in the emission spectra was observed for the cis isomer 3 across all media compared to 7. This behaviour implies that the electronic coupling between D and A is stronger in the cis configuration than that in the trans configuration, likely a function of secondary p-p interactions in the former.”*

3. Page 2, right column, the authors claimed that the high intensity absorption band at 311 nm was assigned to the ICT transition from D to A through the PCP. Generally, the ICT absorption band is usually pretty weak in common TADF molecules. This strong absorption band at 311 nm could be a LE transition from D and/or A. It is strongly commended that the authors provided more data to support this claim.

*To support our claim, we examined the nature and character of transitions around 311 nm with the help of TD-DFT data. We found that the transition at 311 nm has contributions from  $H \rightarrow L$ ,  $H \rightarrow L+2$  and  $H \rightarrow L+5$ , where H is the HOMO and L is the LUMO of the molecule. In both isomers, transitions from  $H \rightarrow L$  and  $H \rightarrow L+2$  have the major contribution of 76% and are charge transfer in nature. The transition from  $H \rightarrow L+5$  has a minor contribution of 4%, which is of LE character localized on the donor moiety. Thus, based on these observations, we assigned the strong absorption band at 311 nm to the ICT transition from D to A through PCP. We have added the natural transition orbital diagrams of  $L+2$  and  $L+5$  to ESI (figure S4). We have added the following text in the main manuscript (page 2)*

*“Both isomers possess a high intensity absorption band at 311 nm, which was assigned to the ICT transition from D to A through the PCP based on TD-DFT calculations (Figure S4).”*

4. Page 3, right column, the experimental  $\Delta E_{ST}$  was underestimated when  $S_1$  was calculated by room temperature fluorescence spectra, while  $T_1$  was estimated from 77 K phosphorescence spectra. It is strongly recommended that the authors recalculated the  $\Delta E_{ST}$  values of these new compounds.

*We have recalculated the  $\Delta E_{ST}$  for both the isomers from the onset of prompt and delayed spectra measured at 77K in 15 wt.% doped films in mCP.  $\Delta E_{ST}$  values of 0.13 eV and 0.17 eV were observed for 3 and 7 respectively. We have updated the figure 4 and the corresponding text in the main manuscript.*

*The text now reads “The  $\Delta E_{ST}$  of 3 and 7 were determined from the singlet and triplet energies estimated from the onset of the prompt and delayed emission spectra, respectively, measured in 15 wt% mCP doped films at 77 K (Fig 4). Both isomers exhibited high singlet energies coupled with small  $\Delta E_{ST}$  values of 0.13 eV and 0.17 eV for 3 and 7, respectively, confirming their TADF character.”*

Tel: +44 1334 463826; Fax: +44 1334 463808; [eli.zysman-colman@st-andrews.ac.uk](mailto:eli.zysman-colman@st-andrews.ac.uk); <http://www.zysman-colman.com>

5. If possible, the authors could employ these two TADF emitters in OLED to check how the devices work.

***Please see our response to point 4 of referee 1***

6. Page 3, right column, the caption of Figure 5 and the main text should be separated.

***We have separated the caption of Figure 5 (page 3) from the main text.***

7. Page 3, right column, for the transient PL part, it is strongly recommended that the authors provide fitting curves and parameters for the transient PL curves of both emitters.

***We have added the Updated figures and fitting parameters to ESI (Figure S2, page S21).***

8. Page 3, left column, wt% should be wt.%.  
Typo:

***We have replaced wt% with wt.% throughout the manuscript.***

---

Sincerely,



Eli Zysman-Colman



Journal Name

COMMUNICATION

## (Deep) Blue Through-Space Conjugated TADF Emitters Based on [2.2]Paracyclophanes

Received 00th January 20xx,  
Accepted 00th January 20xxEduard Spuling,<sup>‡a</sup> Nidhi Sharma,<sup>‡b,c</sup> Ifor D. W. Samuel,<sup>c\*</sup> Eli Zysman-Colman,<sup>b\*</sup> and Stefan Bräse<sup>a,d\*</sup>

DOI: 10.1039/x0xx00000x

www.rsc.org/

The first examples of through-space conjugated thermally activated delayed fluorescence (TADF) emitters based on a [2.2]paracyclophane (PCP) skeleton with stacked (coplanar) donor-acceptor groups have been synthesized. The optoelectronic properties are studied by the relative configuration, *cis* (pseudo-geminal) and *trans* (pseudo-para), of the donor and acceptor groups.

Thermally activated delayed fluorescence (TADF) is now regarded as the most promising mechanism for harvesting excitons<sup>1</sup> in electroluminescent devices and has thus garnered much attention in organic light-emitting diode (OLED) research following the seminal works of Adachi *et al.*<sup>2–5</sup> A small energy gap ( $\Delta E_{ST}$ ) between the singlet and triplet excited states permits rapid effective equilibration between the two via intersystem crossing (ISC) and reverse intersystem crossing (rISC), evidenced by an observed thermally promoted delayed fluorescence upon photo- or electrical excitation.<sup>1, 6</sup> A small  $\Delta E_{ST}$  is achieved through a small exchange integral between frontier molecular orbitals; however, this has the potential to compromise the photoluminescence quantum yield ( $\Phi_{PL}$ ) by reducing the oscillator strength of the transition. Therefore, strict design principles must be followed to produce bright and efficient TADF emitters.<sup>7</sup> Although the vast majority of reported TADF emitters adhere to the design paradigm of molecules containing donors and acceptors possessing a highly twisted relative conformation in order to minimize the

exchange integral, recent findings indicate that planar structures can exhibit TADF as well while maintaining a strong oscillator strength.<sup>8, 9</sup> These examples demonstrate that the mechanism of and design rules governing TADF are still ripe for continuing investigation.<sup>10</sup> Another striking design concept for TADF that has been explored by Swager, Baldo *et al.* is the electronic communication of donor and acceptor groups mediated by through-space conjugation either using a triptycene skeleton confining the donor and acceptor units in a 120° orientation,<sup>11</sup> or a xanthene-linked cofacial disposition of donor (D) and acceptor (A) with a distance of 3.3–3.5 Å.<sup>12</sup> Although TADF was observed with delayed lifetimes,  $\tau_D$  between 2.0–3.0  $\mu$ s and moderate  $\Phi_{PL}$  in this latter report, the through-space electronic communication mainly occurred via C–H $\cdots$  $\pi$  interactions, creating efficient aggregation induced emission.

The [2.2]paracyclophane (PCP) is a compact skeleton confining two benzene rings (“decks”) by ethylene bridges in a coplanar, though slightly bent and configurationally stable, conformation with a deck distance of 3.09 Å,<sup>13</sup> which is smaller than the van der Waals distance between layers of graphite (3.35 Å). This enables a stronger transannular electronic communication between the benzene decks. This model compound for  $\pi$ – $\pi$  transannular interaction sparked numerous investigations over the last decades. For instance, Bazan *et al.* investigated D–A stilbene derivatives based on PCP that exhibited nonlinear optical properties and significant through-space charge transfer,<sup>14, 15</sup> including strong positive solvatochromism caused by a polarizable electronic structure in the excited state.<sup>16</sup> Morisaki, Chujo *et al.* focused on PCP-based through-space  $\pi$ -extended conjugated polymers, demonstrating that electronic interactions can be effective through more than ten layers in the ground state, yet emission in these systems occurs from the isolated monomer  $\pi$  systems, giving access to well-defined monomer-localized HOMO–LUMO gaps rather than a broad valence-conduction band gap in the polymers.<sup>17, 18</sup> Additionally, given the inherent planar chirality in PCPs, this scaffold can yield chromophores with intense circular polarized luminescence.<sup>19–22</sup> Despite these fascinating properties, PCP

<sup>a</sup> Institute of Organic Chemistry, Karlsruhe Institute of Technology (KIT), Fritz-Haber-Weg 6, 76131 Karlsruhe, Germany. Fax: (+49)-721-6084-8581; phone: (+49)-721-6084-2903; E-mail: braese@kit.edu

<sup>b</sup> Organic Semiconductor Centre, EaStCHEM School of Chemistry, University of St Andrews, St Andrews, Fife, KY16 9ST, UK. E-mail: eli.zysman-colman@st-andrews.ac.uk; Web: <http://www.zysman-colman.com>; Tel: +44 (0)1334 463826

<sup>c</sup> Organic Semiconductor Centre, SUPA, School of Physics and Astronomy, University of St Andrews, North Haugh, St Andrews, KY16 9SS, U.K. E-mail: idws@st-andrews.ac.uk

<sup>d</sup> Institute of Toxicology and Genetics, Karlsruhe Institute of Technology (KIT), Hermann-von-Helmholtz-Platz 1, D-76344 Eggenstein-Leopoldshafen, Germany.

‡ These authors contributed equally to this work.  
Electronic Supplementary Information (ESI) available: [details of any supplementary information available should be included here]. See DOI: 10.1039/x0xx00000x

## COMMUNICATION

Journal Name

chemistry suffers from challenging or sometimes unpredictable reactivity. Although various successful cross-coupling protocols have been reported,<sup>23</sup> a direct C-N coupling to a *N*-heterocycle such as carbazole (Cz) or diphenylamine (DPA), though claimed in numerous patents,<sup>24, 25</sup> has never been reported in the scientific literature thus far.

In this communication we report the first examples of thermally activated delayed fluorescence enabled by through-space conjugation of a [2.2]paracyclophane skeleton (Fig. 1).

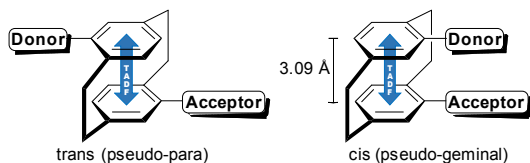
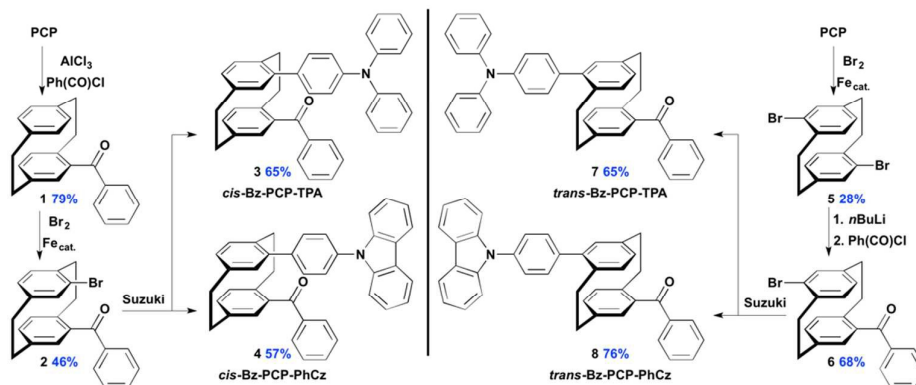


Figure 1 Concept of through-space conjugation of a [2.2]paracyclophane skeleton for thermally activated delayed fluorescence (TADF).

In order to obtain both the *cis* and *trans* isomers (pseudo-geminal and pseudo-para in PCP terminology, see Figure S1), two different approaches were investigated (Scheme 1). Compound **2** was synthesized by Friedel-Craft acylation of PCP and subsequent exploitation of the transannular directing effect to selectively target the pseudo-geminal position of the carbonyl group towards electrophilic aromatic bromination.<sup>26</sup> The *trans* (pseudo-para) intermediate **6** was obtained by monolithiation<sup>14</sup> of the highly insoluble pseudo-para dibromide **5** followed by quenching with benzoyl chloride. The intermediates **2** and **6** possess benzoyl acceptor groups<sup>27-29</sup> and a bromo-functionalized building block suitable for cross-coupling of various donor groups. Targeting deep blue emitters, relatively weak donors (4'-*N*,*N*-diphenylamino)phenyl and (4'-*N*-carbazolyl)phenyl were installed via optimized Suzuki-Miyaura protocols (ESI) in moderate to good yields.



Scheme 1 [2.2]paracyclophane (PCP) based through-space conjugated benzoyl acceptor TADF systems. Left: Synthesis of pseudo-geminal (*cis*) TADF systems. Right: Synthesis of pseudo-para (*trans*) TADF systems. All molecules were prepared in a racemic fashion.

Density functional theory (DFT) calculations were performed in the gas phase to assess the electronic structures of both *cis* and *trans* derivatives (see ESI for details). The  $S_1$  and  $T_1$  excited states were calculated from the optimized ground state structure using the Tamm-Dancoff approximations<sup>30, 31</sup> (TDA) to TD-DFT. Focusing on the DPA derivatives, Fig. 2, the highest occupied molecular orbitals (HOMO) and lowest unoccupied molecular orbitals (LUMO) for **3** and **7** are mainly localized over the donor and acceptor moieties and the adjoining benzene deck, respectively. The strong transannular electronic communication mediated by the PCP core promotes an efficient through space intramolecular charge transfer (ICT) while the inherent rigidity of the PCP was expected to minimize the vibrational motion of the molecule thereby reducing non-radiative decay pathways. The well separated frontier orbitals resulted in small calculated  $\Delta E_{ST}$  values of 0.04 eV and 0.19 eV for **3** and **7**, respectively, coupled with high excited singlet energies ( $S_1$  state), suggesting their strong potential as deep blue TADF emitters. Upon changing the donor group to the weaker carbazole, relatively large  $\Delta E_{ST}$  values of 0.32 eV and 0.46 eV for isomers **4** and **8**, respectively, were observed (Fig. S2). No further studies were carried out

for isomer **4** and **8**. Figure 3a shows the UV-Vis absorption and photoluminescence (PL) spectra of **3** and **7** in toluene and the data are summarized in Table 1. Both isomers possess a high intensity absorption band at 311 nm, which was assigned to the ICT transition from D to A through the PCP based on TD-DFT calculations (Fig. S4).

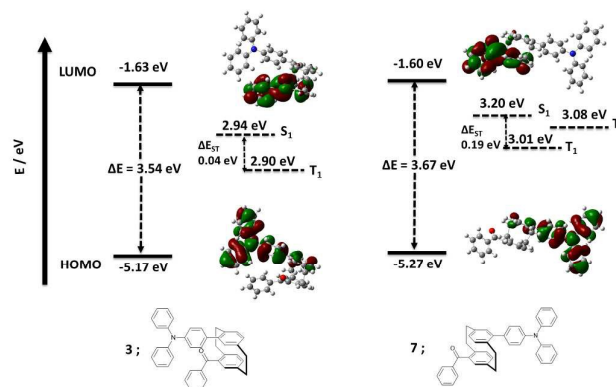


Figure 2. HOMO-LUMO profiles and excited state dynamics of *cis* and *trans* isomers **3** and **7**, respectively (pbe0/6-31G(d,p)).

In the PL spectra in PhMe, both isomers exhibited two distinct bands. The high energy band centred at 410 nm and 404 nm for **3** and **7**, respectively, was assigned to the “phane state” formed between two benzene decks of PCP scaffold.<sup>32, 33</sup> The low energy band at 492 nm for **3** and 455 nm for **7** was attributed to the ICT transition between donor and acceptor moieties. Photoluminescence quantum yields,  $\Phi_{\text{PL}}$ , in PhMe for **3** and **7** were 45% and 60%, which decreased to 30% and 42%, respectively, upon exposure to air. Time-resolved PL spectra (Fig. S1), however, do not show a delayed emission lifetime component, which would suggest that the TADF mechanism in solution is either not present or very weak.

We next investigated the solid-state PL behaviour of both derivatives in doped thin films (Fig. 3b). In the thin film, both derivatives exhibited an unstructured emission profile, characteristic of an excited state with significant ICT character.

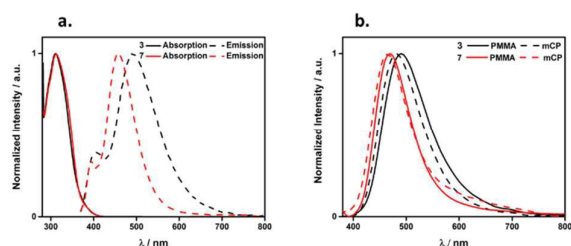
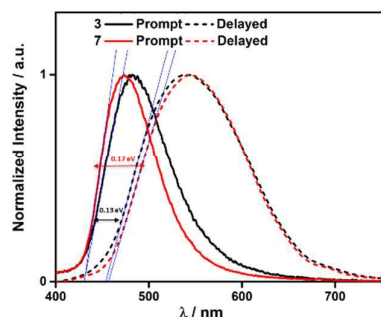


Figure 3. a.) UV-Vis and PL spectra in degassed PhMe and b.) PL spectra in 10 wt.% doped films in PMMA and 15 wt.% doped films in mCP of **3** (black) and **7** (red).  $\lambda_{\text{exc}} = 360$  nm.

In 10 wt.% doped solution-processed films in PMMA, **3** showed sky-blue emission with  $\lambda_{\text{PL}}$  of 485 nm while the emission of **7** was slightly blue-shifted at 470 nm in strong agreement with the calculated  $S_1$  energies. Both isomers exhibited a prompt lifetime,  $\tau_{\text{p}}$ , of 19 ns (for **3**) and 10 ns (for **7**), followed by a very short delayed component,  $\tau_{\text{D}}$  of 0.7  $\mu\text{s}$  and 1.6  $\mu\text{s}$  for **3** and **7**, respectively. However, the  $\Phi_{\text{PL}}$  of the PMMA films of both the isomers remained low, close to 5% for **3** and 7.5% for **7**. With a view to employing these compounds as emitters in OLEDs, we next studied the emitters in the high triplet energy host, 1,3-bis(*N*-carbazolyl)benzene, mCP, with a vacuum-deposited doping concentration of 15 wt.%. The emission maxima were slightly blue-shifted at 480 and 465 nm for **3** and **7**, respectively, with strongly reduced  $\Phi_{\text{PL}}$  of 12 and 15%, respectively, compared to solution-state measurements. Reducing the doping concentration to 1 wt.% resulted in reduced  $\Phi_{\text{PL}}$  of 7% for both isomers (Table S1). The optoelectronic properties of **3** and **7** are influenced by the relative configuration of D and A. A red-shift in the emission spectra was observed for the *cis* isomer **3** across all media compared to **7**. This behaviour implies that the electronic coupling between D and A is stronger in the *cis* configuration than that in the *trans* configuration, likely a function of secondary  $\pi$ - $\pi$  interactions in the former.

The  $\Delta E_{\text{ST}}$  of **3** and **7** were determined from the singlet and triplet energies estimated from the onset of the prompt and delayed emission spectra, respectively, measured in 15 wt.% mCP doped films at 77 K (Fig 4). Both isomers exhibited high



singlet energies coupled with small  $\Delta E_{\text{ST}}$  values of 0.13 eV and 0.17 eV for **3** and **7**, respectively, confirming their TADF character.

Figure 4. Prompt and delayed (by 50  $\mu\text{s}$ , 200  $\mu\text{s}$  window) spectra of **3** and **7** in 15 wt.% mCP doped films, measured at 77 K. ( $\lambda_{\text{exc}} = 378$  nm)

Transient PL measurements in 15 wt.% mCP doped films revealed biexponential decay kinetics. Both isomers exhibited a prompt lifetime,  $\tau_{\text{p}}$ , of 17 ns (for **3**) and 7.4 ns (for **7**) and a very short delayed lifetime,  $\tau_{\text{D}}$ , of 1.8  $\mu\text{s}$  (for **3**) and 3.6  $\mu\text{s}$  (for **7**). Furthermore, rates of reverse intersystem crossing,  $k_{\text{rISC}}$  were found to be  $7.0 \times 10^5 \text{ s}^{-1}$  and  $3.1 \times 10^5 \text{ s}^{-1}$  for **3** and **7**, respectively (Table S2, ESI). Such short  $\tau_{\text{D}}$  and large  $k_{\text{rISC}}$  values are characteristics of an efficient rISC mechanism. Despite the desirable blue emission and short delayed lifetimes, the  $\Phi_{\text{PL}}$  of these emitters remained poor. We investigated a range of high-energy host materials, such as DPEPO and CzSi, and doping concentrations (from 1-25 wt.%) in an effort to enhance the  $\Phi_{\text{PL}}$  in the solid state; however, the highest  $\Phi_{\text{PL}}$  values were found in mCP at 15 wt.% (Table S1).

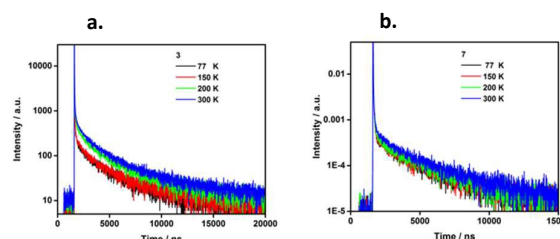


Figure 5. Temperature dependence of delayed lifetime of a.) **3** and b.) **7**.  $\lambda_{\text{exc}} = 378$  nm.

To further corroborate the TADF nature of these emitters, we investigated the temperature dependence of the delayed lifetimes (Fig. 5). For both compounds, the intensity of delayed emission gradually increases with increasing temperature, providing direct evidence of TADF.

Table 1. Photophysical properties of **3** and **7**.

	$\lambda_{\text{abs}}^a$ / nm	$\lambda_{\text{PL}}^a$ / nm	$\Phi_{\text{PL}}^b$ / %	$\Phi_{\text{PL}}^c$ / %	$\tau_{\text{p}}^d$ / ns	$\tau_{\text{D}}^d$ / $\mu\text{s}$
<b>3</b> (cis)	311	480	45 (30)	12	17 (0.88)	1.8 (0.12)
<b>7</b> (trans)	312	465	60 (42)	15	7.4 (0.44)	3.6 (0.56)

<sup>a</sup> In degassed PhMe at 298 K. <sup>b</sup> 0.5 M quinine sulfate in H<sub>2</sub>SO<sub>4</sub> (aq) was used as the reference ( $\Phi_{\text{PL}}$ : 54.6%,  $\lambda_{\text{exc}}$ : 360 nm). <sup>c</sup> Values quoted are in degassed solutions, which were prepared by three freeze-pump-thaw cycles. Values in parentheses are for aerated solutions, which were prepared by bubbling air for 10 min. <sup>d</sup> Thin films were prepared by vacuum depositing 15 wt.% doped samples in mCP and values were determined using an integrating sphere ( $\lambda_{\text{exc}}$ : 360 nm); degassing was done by N<sub>2</sub> purge. Values in parentheses are the pre-exponential weighting factors, determined in 15 wt.% mCP doped films of **3** and **7** ( $\lambda_{\text{exc}}$ : 378 nm).

In conclusion, we have developed the first examples of TADF emitters incorporating a PCP core, which we exploited to mediate electronic communication between donor and acceptor groups on adjoining benzene decks. Both the *cis* and *trans* isomers exhibited blue TADF emission and short delayed lifetimes in the range of 1–3  $\mu\text{s}$ . These compounds unfortunately possess low photoluminescence quantum yields in the solid state. We are presently investigating modified designs to mitigate this issue such that paracyclophane-based TADF emitters can be incorporated into OLED devices.

### Conflicts of interest

There are no conflicts to declare.

### Acknowledgements

E. S. and S. B. acknowledge funding from DFG in the frame of SFB1176 (projects A4, B3 and C6) and KSOP (fellowship to E. S.). E. Z.-C. and I. D. W. S. thank the Engineering and Physical Sciences Research Council (EPSRC) (No. EP/P010482/1) for financial support. I.D.W.S. also acknowledges support from a Royal Society Wolfson Research Merit Award. We thank the EPSRC UK National Mass Spectrometry Facility at Swansea University for analytical services.

### Notes and references

- M. Y. Wong and E. Zysman-Colman, *Adv. Mater.*, 2017, **29**, 1605444.
- A. Endo, M. Ogasawara, A. Takahashi, D. Yokoyama, Y. Kato and C. Adachi, *Adv. Mater.*, 2009, **21**, 4802-4806.
- A. Endo, K. Sato, K. Yoshimura, T. Kai, A. Kawada, H. Miyazaki and C. Adachi, *Appl. Phys. Lett.*, 2011, **98**, 42.
- H. Uoyama, K. Goushi, K. Shizu, H. Nomura and C. Adachi, *Nature*, 2012, **492**, 234-238.

- Q. Zhang, J. Li, K. Shizu, S. Huang, S. Hirata, H. Miyazaki and C. Adachi, *J. Am. Chem. Soc.*, 2012, **134**, 14706-14709.
- Z. Yang, Z. Mao, Z. Xie, Y. Zhang, S. Liu, J. Zhao, J. Xu, Z. Chi and M. P. Aldred, *Chem. Soc. Rev.*, 2017, **46**, 915-1016.
- Y. Im, M. Kim, Y. J. Cho, J. A. Seo, K. S. Yook and J. Y. Lee, *Chem. Mater.*, 2017, **29**, 1946-1963.
- T. Hatakeyama, K. Shiren, K. Nakajima, S. Nomura, S. Nakatsuka, K. Kinoshita, J. Ni, Y. Ono and T. Ikuta, *Adv. Mater.*, 2016, **28**, 2777-2781.
- X. K. Chen, Y. Tsuchiya, Y. Ishikawa, C. Zhong, C. Adachi and J. L. Bredas, *Adv. Mater.*, 2017, **29**, 1702767.
- T. J. Penfold, F. B. Dias and A. P. Monkman, *Chem. Commun.*, 2018, **54**, 3926-3935.
- K. Kawasumi, T. Wu, T. Zhu, H. S. Chae, T. Van Voorhis, M. A. Baldo and T. M. Swager, *J. Am. Chem. Soc.*, 2015, **137**, 11908-11911.
- H. Tsujimoto, D. G. Ha, G. Markopoulos, H. S. Chae, M. A. Baldo and T. M. Swager, *J. Am. Chem. Soc.*, 2017, **139**, 4894-4900.
- D. J. Cram and J. M. Cram, *Acc. Chem. Res.*, 1971, **4**, 204-213.
- J. Zyss, I. Ledoux, S. Volkov, V. Chernyak, S. Mukamel, G. P. Bartholomew and G. C. Bazan, *J. Am. Chem. Soc.*, 2000, **122**, 11956-11962.
- G. P. Bartholomew and G. C. Bazan, *Acc. Chem. Res.*, 2001, **34**, 30-39.
- J. W. Hong, H. Y. Woo, B. Liu and G. C. Bazan, *J. Am. Chem. Soc.*, 2005, **127**, 7435-7443.
- Y. Morisaki and Y. Chujo, *Polym. Chem.*, 2011, **2**, 1249-1257.
- Y. Morisaki and Y. Chujo, *Chem. Lett.*, 2012, **41**, 840-846.
- Y. Morisaki, M. Gon, T. Sasamori, N. Tokitoh and Y. Chujo, *J. Am. Chem. Soc.*, 2014, **136**, 3350-3353.
- M. Gon, Y. Morisaki, R. Sawada and Y. Chujo, *Chemistry*, 2016, **22**, 2291-2298.
- M. Gon, Y. Morisaki and Y. Chujo, *Chem. Commun.*, 2017, **53**, 8304-8307.
- M. Gon, R. Sawada, Y. Morisaki and Y. Chujo, *Macromolecules*, 2017, **50**, 1790-1802.
- C. Braune, E. Spuling, N. B. Heine, M. Cakici, M. Nieger and S. Bräse, *Adv. Synth. Catal.*, 2016, **358**, 1664-1670.
- K.-J. Yoon, H.-J. Noh, D.-W. Yoon, I.-A. Shin and J.-Y. Kim, *EP3029753B1*.
- S. L. Buchwald and W. Huang, *US20160359118A1*.
- H. J. Reich and D. J. Cram, *J. Am. Chem. Soc.*, 1968, **90**, 1365-8.
- S. Y. Lee, T. Yasuda, Y. S. Yang, Q. Zhang and C. Adachi, *Angew. Chem. Int. Ed. Engl.*, 2014, **53**, 6402-6406.
- P. Rajamalli, D. R. Martir and E. Zysman-Colman, *ACS Appl. Energy Mater.*, 2018, **1**, 649-654.
- R. P. Gounder, D. R. Martir and E. Zysman-Colman, *J. Photon. Energy*, 2018, **8**, 032106.
- J. P. Perdew, M. Emzerhof and K. Burke, *J. Chem. Phys.*, 1996, **105**, 9982-9985.
- S. Grimme, *Chem. Phys. Lett.*, 1996, **259**, 128-137.
- E. Elacqua and L. R. MacGillivray, *Eur. J. Org. Chem.*, 2010, **2010**, 6883-6894.
- J. L. Zafra, A. Molina Ontoria, P. Mayorga Burrezo, M. Pena-Alvarez, M. Samoc, J. Szeremeta, F. J. Ramirez, M. D. Lovander, C. J. Droske, T. M. Pappenfus, L. Echegoyen, J. T. Lopez Navarrete, N. Martin and J. Casado, *J. Am. Chem. Soc.*, 2017, **139**, 3095-3105.
- W. H. Melhuish, *J. Phys. Chem.*, 1961, **65**, 229-235.

# (Deep) Blue Through-Space Conjugated TADF Emitters Based on [2.2]Paracyclophanes

*Eduard Spuling,<sup>‡a</sup> Nidhi Sharma,<sup>‡b,c</sup> Ifor D. W. Samuel,<sup>c\*</sup> Eli Zysman-Colman,<sup>b\*</sup> and Stefan Bräse<sup>a,d\*</sup>*

<sup>a</sup> Institute of Organic Chemistry, Karlsruhe Institute of Technology (KIT), Fritz-Haber-Weg 6, 76131 Karlsruhe, Germany. Fax: (+49)-721-6084-8581; phone: (+49)-721-6084-2903; E-mail: [braese@kit.edu](mailto:braese@kit.edu)

<sup>b</sup> Organic Semiconductor Centre, EaStCHEM School of Chemistry, University of St Andrews, St Andrews, Fife, KY16 9ST, UK. E-mail: [eli.zysman-colman@st-andrews.ac.uk](mailto:eli.zysman-colman@st-andrews.ac.uk); Web: <http://www.zysman-colman.com>; Fax:+44 (0)1334 463808; Tel:+44 (0)1334 463826

<sup>c</sup> Organic Semiconductor Centre, SUPA, School of Physics and Astronomy, University of St Andrews, North Haugh, St Andrews, KY16 9SS, U.K. E-mail: [idws@st-andrews.ac.uk](mailto:idws@st-andrews.ac.uk)

<sup>d</sup> Institute of Toxicology and Genetics, Karlsruhe Institute of Technology (KIT), Hermann-von-Helmholtz-Platz 1, D-76344 Eggenstein-Leopoldshafen, Germany.

## Table of Contents

Additional Information .....	2
2. Synthesis of Compounds .....	3
2.1. General Remarks.....	3
2.2. Synthetic Procedures and Analytical Data.....	4
3. Photophysical Characterization .....	20
4. DFT modelling.....	23
5. References.....	38

## Additional Information

### Nomenclature of [2.2]Paracyclophanes

The IUPAC nomenclature for cyclophanes in general is confusing.<sup>1</sup> Therefore Vögtle *et al.* developed a specific cyclophane nomenclature, which is based on a core-substituent ranking.<sup>2</sup> This is exemplified in Figure S1 for the [2.2]paracyclophane.

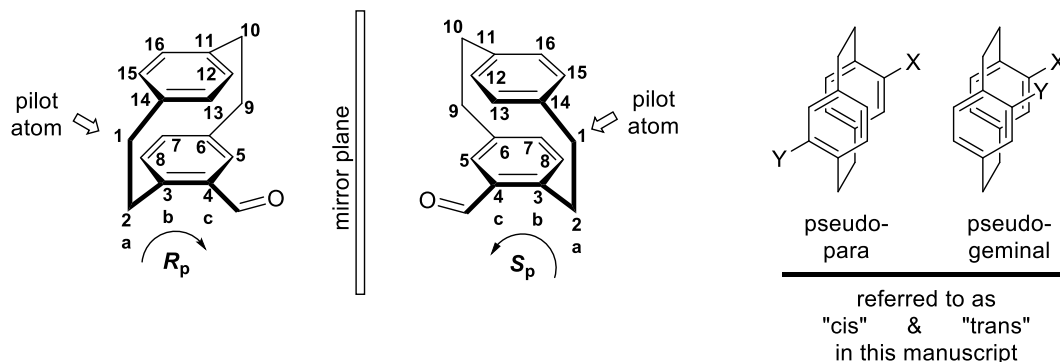


Figure S1. Entire nomenclature shown on both 4-formyl[2.2]paracyclophane enantiomers.

The core structure is named according to the length of the aliphatic bridges in squared brackets (e.g. [n.m]) and the benzene substitution patterns (ortho, meta or para). [2.2]Paracyclophane belongs to the  $D_{2h}$  symmetry, which is broken by the first substituent, resulting in two planar chiral enantiomers. They cannot be drawn in a racemic fashion. By definition, the arene bearing the substituent is set to a chirality plane, and the first atom of the cyclophane structure outside the plane and closest to the chirality center is defined as the “*pilot atom*”. If both arenes are substituted, the substituent with higher priority according to the Cahn-Ingold-Prelog (CIP) nomenclature is preferred.<sup>3</sup> The stereo descriptor is determined by the sense of rotation viewed from the pilot atom. To describe the positions of the substituents correctly, an unambiguous numeration is needed. The numbering of the arenes follows the sense of rotation determined by CIP. To indicate the planarity of the chiral center, a subscripted  $p$  is added. Unfortunately the numbering of the second arene is not consistent in the literature. Therefore another description based on the benzene substitution patterns is preferred for disubstituted [2.2]paracyclophanes. Substitution on the other ring is commonly named pseudo-(*ortho*, *meta*, *para* or *geminal*). With respect to the scope and aim of this communication pseudo-*para* (4,16) derivatives are named “trans” and pseudo-*geminal* (4,13) derivatives “cis”.

## 2. Synthesis of Compounds

### 2.1. General Remarks

NMR spectra were recorded on a *Bruker* AM 400 or a *Bruker* Avance 500 spectrometer as solutions at room temperature. Chemical shifts  $\delta$  are expressed in parts per million (ppm) downfield from tetramethylsilane (TMS). References for  $^1\text{H}$  NMR and  $^{13}\text{C}$  NMR were the residual solvent peaks of chloroform ( $^1\text{H}$ :  $\delta = 7.26$  ppm), DMSO ( $^1\text{H}$ :  $\delta = 2.50$  ppm),  $\text{D}_1$ -chloroform ( $^{13}\text{C}$ :  $\delta = 77.0$  ppm) and  $\text{D}_6$ -DMSO ( $^{13}\text{C}$ :  $\delta = 39.43$  ppm). All coupling constants ( $J$ ) are absolute values and are expressed in Hertz (Hz). The description of signals includes: s = singlet, d = doublet, t = triplet, q = quartet, quin = quintet, m = multiplet,  $m_c$  = centered multiplet, dd = doublet of doublets and ddd = double doublet of doublets and so forth. The spectra were analyzed according to first order. The assignments of the signal structure in  $^1\text{H}$  NMR were made by the multiplicity and for  $^{13}\text{C}$  NMR by DEPT 90- and DEPT 135-spectra (DEPT = distortionless enhancement by polarization transfer) and are described as follows: + = primary or tertiary C-atom (positive DEPT-signal), - = secondary C-atom (negative signal) and  $\text{C}_{\text{quart.}}$  = quaternary C-atom (no signal).

IR spectra were recorded on a FT-IR *Bruker* IFS 88 spectrometer. The compounds were measured as pure substances by ATR technique (ATR = attenuated total reflection). The position of the absorption band is given in wave numbers  $\tilde{\nu}$  in  $\text{cm}^{-1}$ . The intensities of the bands were characterized as follows: vs = very strong (0–20% T), s = strong (21–40% T), m = medium (41–60% T), w = weak (61–80% T), vw = very weak (81–100% T).

Melting points were measured using a Cambridge Instruments device, model *OptiMelt MPA 100* with a temperature increase of  $1\text{ }^\circ\text{C}/\text{min}$ .

Mass spectra were measured by EI-MS (electron impact mass spectrometry) and were recorded on a *Finnigan MAT 95*. The peaks are given as mass-to-charge-ratio ( $m/z$ ). The molecule peak is given as  $[\text{M}]^+$  and characteristic fragment peaks are given as  $[\text{M-fragment}]^+$  or  $[\text{fragment}]^+$ . The signal intensities are given in percent, relatively to the intensity of the base signal (100%). For the high resolution mass, the following abbreviations were used: calc. = calculated data, found = measured data.

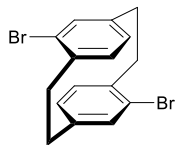
Analytical thin layer chromatography (TLC) was carried out on Merck silica gel coated aluminum plates (silica gel 60,  $\text{F}_{254}$ ), detected under UV-light at 254 nm or stained with “Seebach staining solution” (mixture of molybdate phosphoric acid, cerium(IV)-sulfate tetrahydrate, sulfuric acid and water) or basic potassium permanganate solution. Solvent mixtures are understood as volume/volume. Solvents, reagents and chemicals were purchased from *Sigma-Aldrich*, *ABCR* and *Acros Organics*. All solvents, reagents and chemicals were used as purchased unless stated otherwise.

Air- or moisture-sensitive reactions were carried out under argon atmosphere in oven-dried and previously evacuated glass ware. Liquids were transferred with plastic syringes and steel cannula. Reaction control was

performed by thin layer chromatography. If not stated otherwise, crude products were purified by flash chromatography by the procedure of Still.<sup>4</sup> Silica gel 60 (0.040 × 0.063 mm, Geduran®, Merck) was used as stationary phase and as mobile phase, solvents of p.a. quality were used.

## 2.2. Synthetic Procedures and Analytical Data

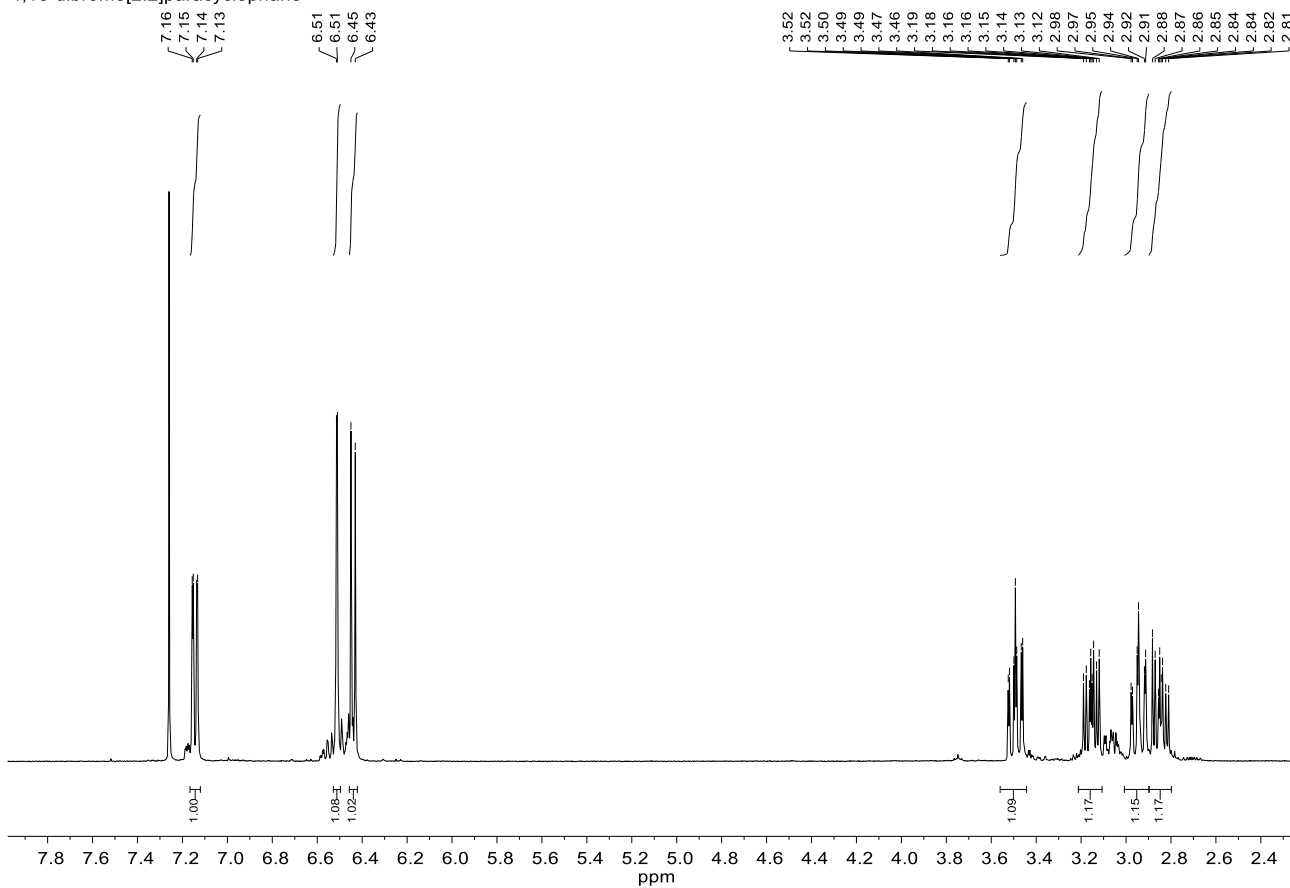
### 4,16-dibromo[2.2]paracyclophane (5):



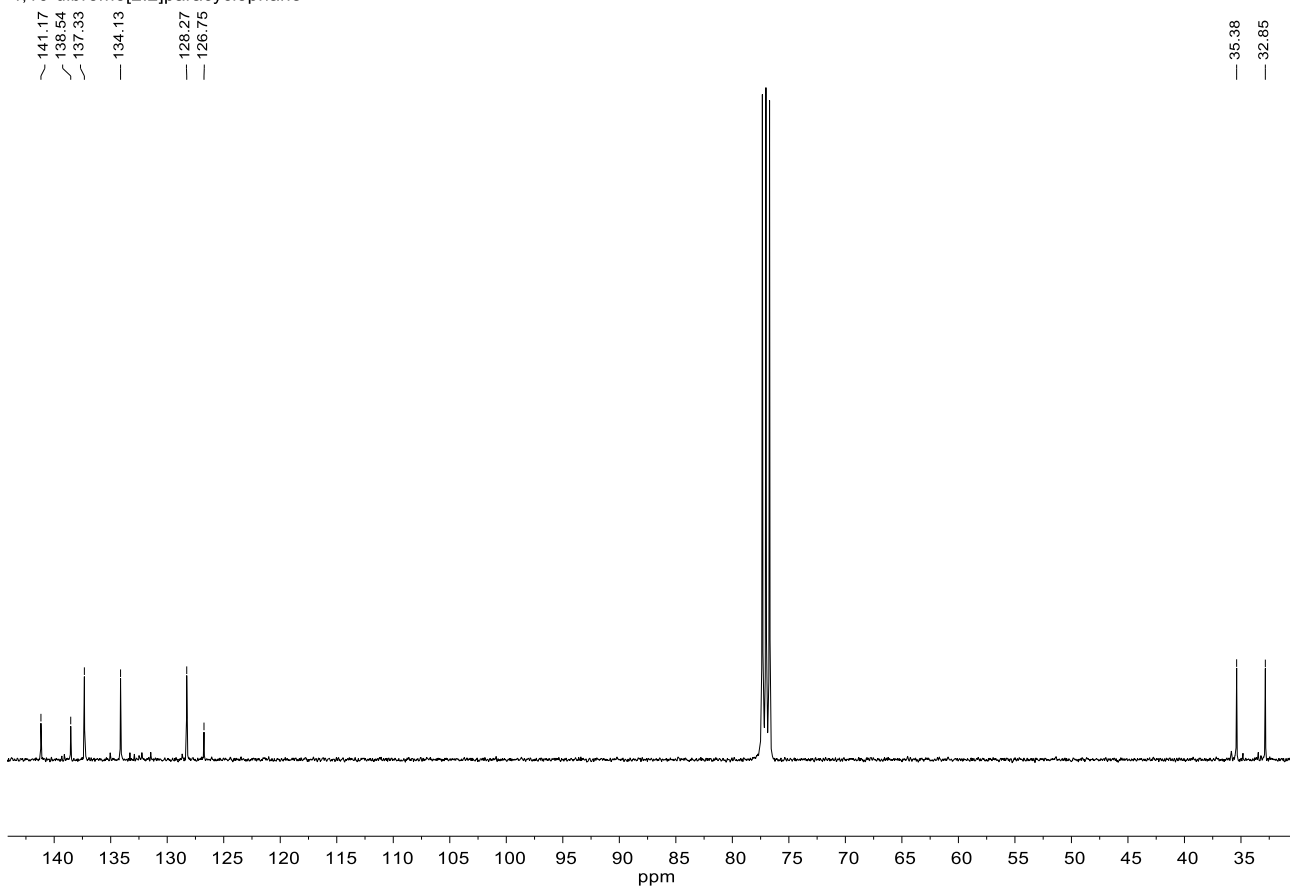
The synthesis followed a modified protocol reported in literature.<sup>5</sup> To iron powder (241 mg, 4.32 mmol, 4.50 mol%) were added 15 mL of a solution of 10.3 mL bromine (32.1 g, 201 mmol, 2.10 equiv.) in 80 mL dichloromethane. After stirring for 1 h, the reaction mixture was diluted with 100 mL dichloromethane and [2.2]paracyclophane (20.0 g, 96.0 mmol, 1.00 equiv.) were added. The mixture was stirred for further 30 min, followed by dropwise addition of the residual bromine solution over 5 h. The reaction mixture was stirred for 3 d. Then a sat. aqueous solution of Na<sub>2</sub>SO<sub>3</sub> was added to the reaction mixture, which was stirred until decoloration occurred (1 h). The organic phase was filtrated and the residual solid dried without further purification. The product was obtained in 9.52 g (26.0 mmol, 28%) as a white solid.

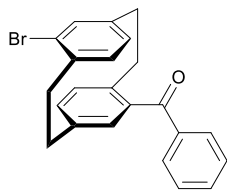
$R_f = 0.72$  (CH/EA 10:1). – <sup>1</sup>H NMR (400 MHz, CDCl<sub>3</sub>):  $\delta = 7.14$  (dd,  $J = 7.8, 1.8$  Hz, 2H), 6.51 (d,  $J = 1.7$  Hz, 2H), 6.44 (d,  $J = 7.8$  Hz, 2H), 3.49 (ddd,  $J = 13.0, J = 10.4, 2.3$  Hz, 2H), 3.15 (ddd,  $J = 12.7, 10.4, 4.9$  Hz, 2H), 2.94 (ddd,  $J = 12.7, 10.7, 2.3$  Hz, 2H), 2.85 (ddd,  $J = 13.2, 10.7, 5.0$  Hz, 2H) ppm. – <sup>13</sup>C NMR (100 MHz, CDCl<sub>3</sub>):  $\delta = 141.3$  (C<sub>quart.</sub>), 138.7 (C<sub>quart.</sub>), 137.5 (+), 134.2 (+), 128.4 (+), 126.9 (C<sub>quart.</sub>), 35.5 (–), 33.0 (–) ppm. – IR (ATR):  $\tilde{\nu} = 2931$  (vw), 2849 (vw), 1582 (vw), 1535 (vw), 1473 (vw), 1449 (vw), 1432 (vw), 1390 (w), 1185 (vw), 1030(w), 898 (w), 855 (w), 829 (w), 706 (w), 669 (w), 648 (w), 464 (w) cm<sup>-1</sup>. – MS (70 eV, EI),  $m/z$  (%): 368/366/364 (19/38/20) [M]<sup>+</sup>, 184/182 (100/95) [M – C<sub>8</sub>H<sub>7</sub>Br]<sup>+</sup>, 103 (19) [C<sub>8</sub>H<sub>7</sub>]<sup>+</sup>. – HRMS (C<sub>16</sub>H<sub>14</sub><sup>79</sup>Br<sub>2</sub>) calc.: 363.9457; found: 363.9457. Analytical data matches that of the literature.<sup>6</sup>

## 4,16-dibromo[2.2]paracyclophane



## 4,16-dibromo[2.2]paracyclophane

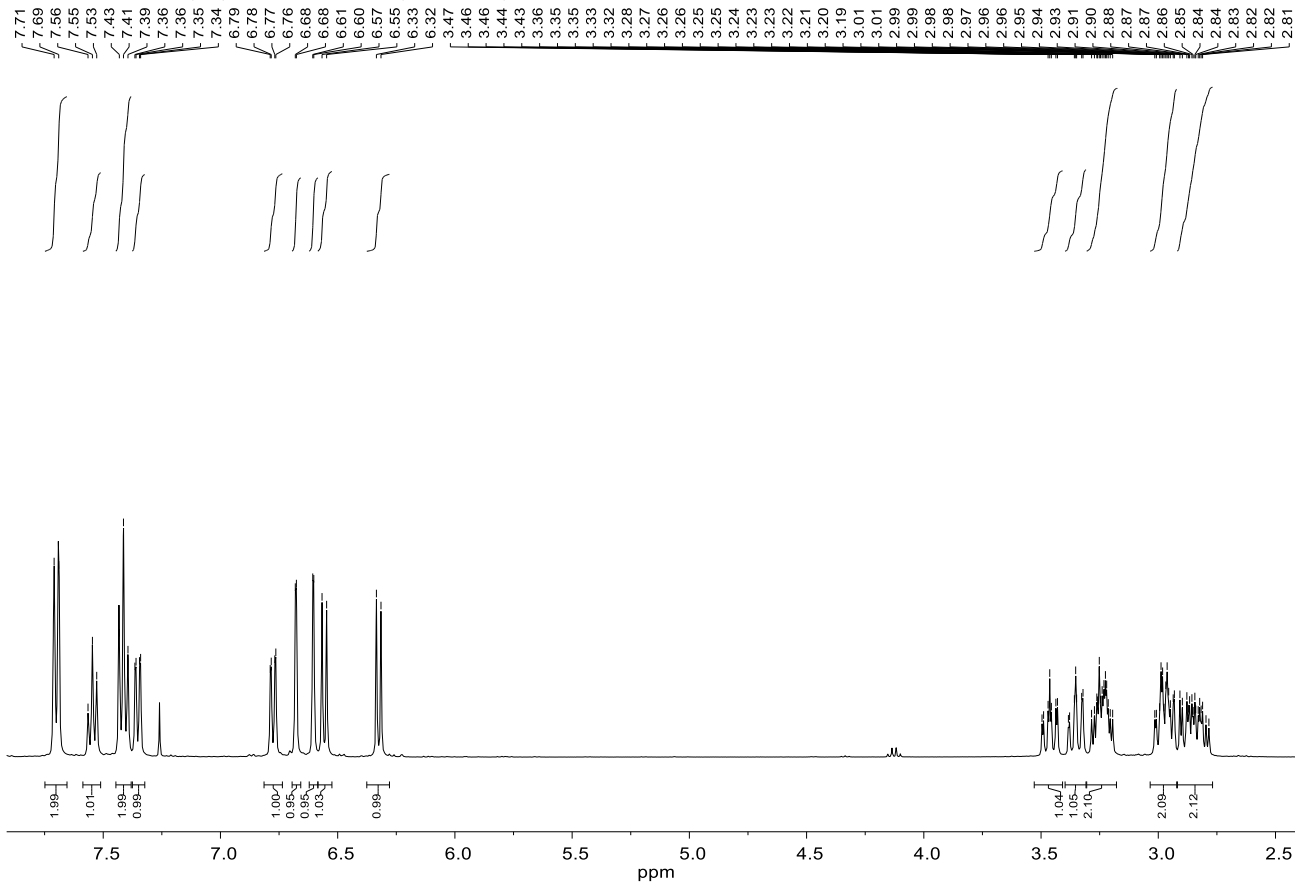


(rac, “trans”) 4 -bromo-16-benzoyl[2.2]paracyclophane (6):

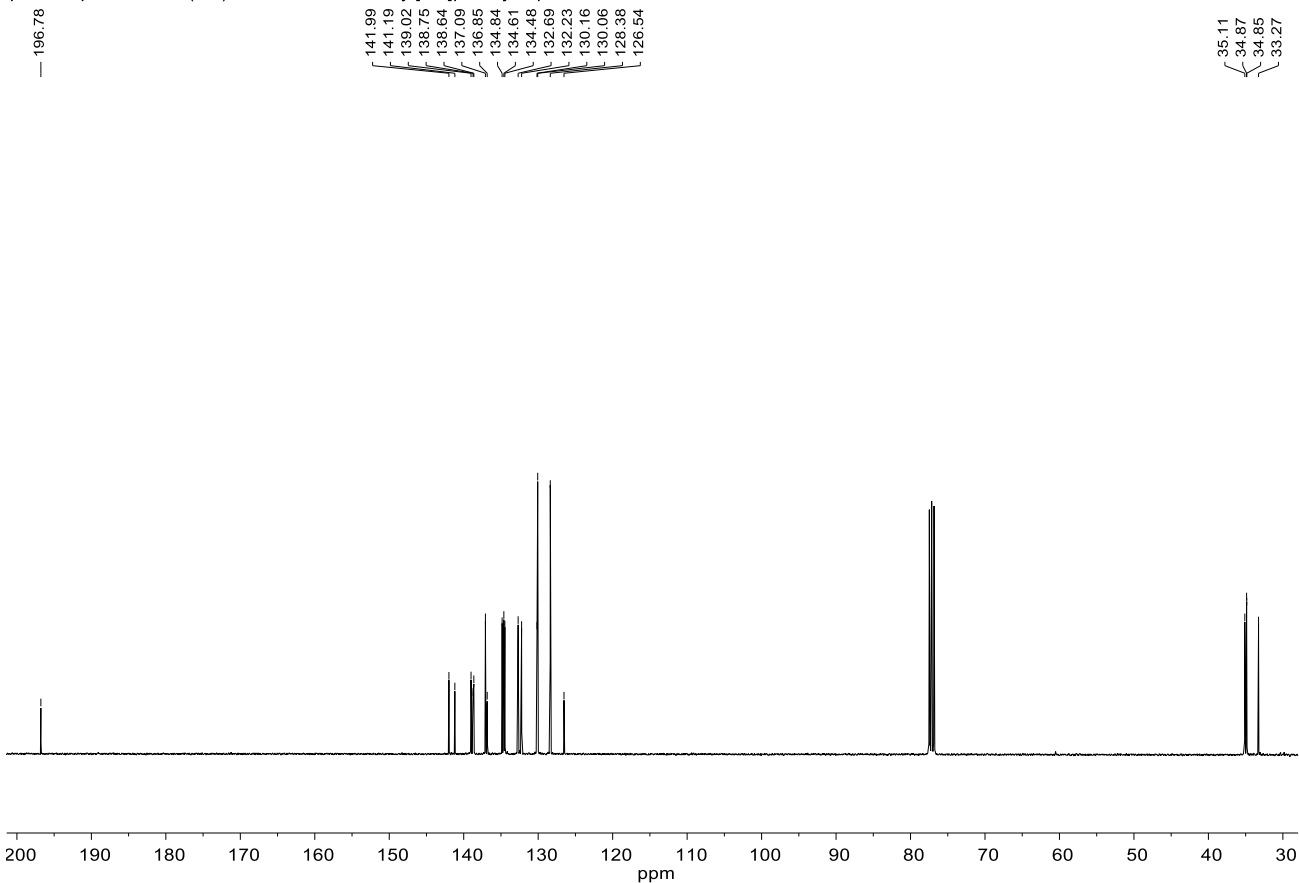
A solution of <sup>n</sup>BuLi (3.94 mL of 2.5 M in hexane, 9.84 mmol, 1.20 equiv.) was added dropwise to a solution of 4,16-dibromo[2.2]paracyclophane (**5**) (3.00 g, 8.20 mmol, 1.00 equiv.) in 150 mL dry tetrahydrofuran at  $-78\text{ }^{\circ}\text{C}$  under argon atmosphere. After stirring for 1 h, the reaction mixture was warmed up to  $0\text{ }^{\circ}\text{C}$  and 7.56 mL of benzoyl chloride (9.22 g, 65.6 mmol, 8.00 equiv.) were added quickly. The reaction mixture was warmed up to room temperature and stirred for 16 h. The reaction mixture was quenched by addition of water and was extracted with ethyl acetate ( $3 \times 100\text{ mL}$ ). The combined organic phases were washed with sat. aqueous  $\text{NH}_4\text{Cl}$  solution (100 mL), brine (100 mL), dried over  $\text{Na}_2\text{SO}_4$  and the solvent was removed under reduced pressure. The crude product was purified by column chromatography (silica gel, cyclohexane/ethyl acetate; 50/1) to yield 4.24 g of an off-white solid (5.58 mmol, 68%).

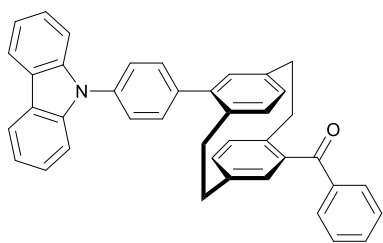
$R_f = 0.22$  (CH/EA 50:1). –  $^1\text{H NMR}$  (400 MHz,  $\text{CDCl}_3$ )  $\delta = 7.70$  (d,  $J = 7.8\text{ Hz}$ , 2H), 7.55 (t,  $J = 7.4\text{ Hz}$ , 1H), 7.41 (t,  $J = 7.4\text{ Hz}$ , 2H), 7.35 (dd,  $J = 7.8, 1.9\text{ Hz}$ , 1H), 6.78 (dd,  $J = 7.9, 1.8\text{ Hz}$ , 1H), 6.68 (d,  $J = 1.9\text{ Hz}$ , 1H), 6.60 (d,  $J = 1.8\text{ Hz}$ , 1H), 6.56 (d,  $J = 7.8\text{ Hz}$ , 1H), 6.33 (d,  $J = 7.8\text{ Hz}$ , 1H), 3.46 (ddd,  $J = 13.2, 10.4, 2.7\text{ Hz}$ , 1H), 3.35 (ddd,  $J = 12.5, 10.5, 2.1\text{ Hz}$ , 1H), 3.28 – 3.19 (m, 2H), 3.01 – 2.93 (m, 2H), 2.92 – 2.76 (m, 2H) ppm. –  $^{13}\text{C NMR}$  (101 MHz,  $\text{CDCl}_3$ )  $\delta = 196.78$  ( $\text{C}_{\text{quat.}}$ , CO), 141.99 ( $\text{C}_{\text{quat.}}$ ), 141.19 ( $\text{C}_{\text{quat.}}$ ), 139.02 ( $\text{C}_{\text{quat.}}$ ), 138.75 ( $\text{C}_{\text{quat.}}$ ), 138.64 ( $\text{C}_{\text{quat.}}$ ), 137.09 (+), 136.85 ( $\text{C}_{\text{quat.}}$ ), 134.84 (+), 134.61 (+), 134.48 (+), 132.69 (+), 132.23(+), 130.16 (+), 130.06 (+), 128.38 (+), 126.54 ( $\text{C}_{\text{quat.}}$ ), 35.11 (–), 34.87 (–), 34.85 (–), 33.27 (–) ppm. – IR (ATR):  $\tilde{\nu} = 2926$  (vw), 1645 (w), 1587 (vw), 1478 (vw), 1448 (vw), 1392 (vw), 1313 (vw), 1279 (w), 1033 (vw), 989 (vw), 908 (vw), 889 (vw), 855 (vw), 822 (w), 742 (w), 722 (vw), 701 (m), 667 (w), 652 (w), 639 (w), 514 (vw), 476 (w), 458 (vw), 397 (vw)  $\text{cm}^{-1}$  – MS (FAB, 3-NBA),  $m/z$ : 391/393 [ $\text{M}(^{79}\text{Br}/^{81}\text{Br})+\text{H}$ ]<sup>+</sup>, 390/392 [ $\text{M}(^{79}\text{Br}/^{81}\text{Br})$ ]<sup>+</sup>. – HRMS ( $\text{C}_{23}\text{H}_{19}^{79}\text{BrO}$ ) calc.: 390.0619; found: 390.0620. – HRMS ( $\text{C}_{23}\text{H}_{19}^{79}\text{BrO}+\text{H}$ ) calc.: 391.0698; found: 391.0700.

## pseudo-para "trans" (rac)-4-bromo-16-benzoyl[2.2]paracyclophane



## pseudo-para "trans" (rac)-4-bromo-16-benzoyl[2.2]paracyclophane

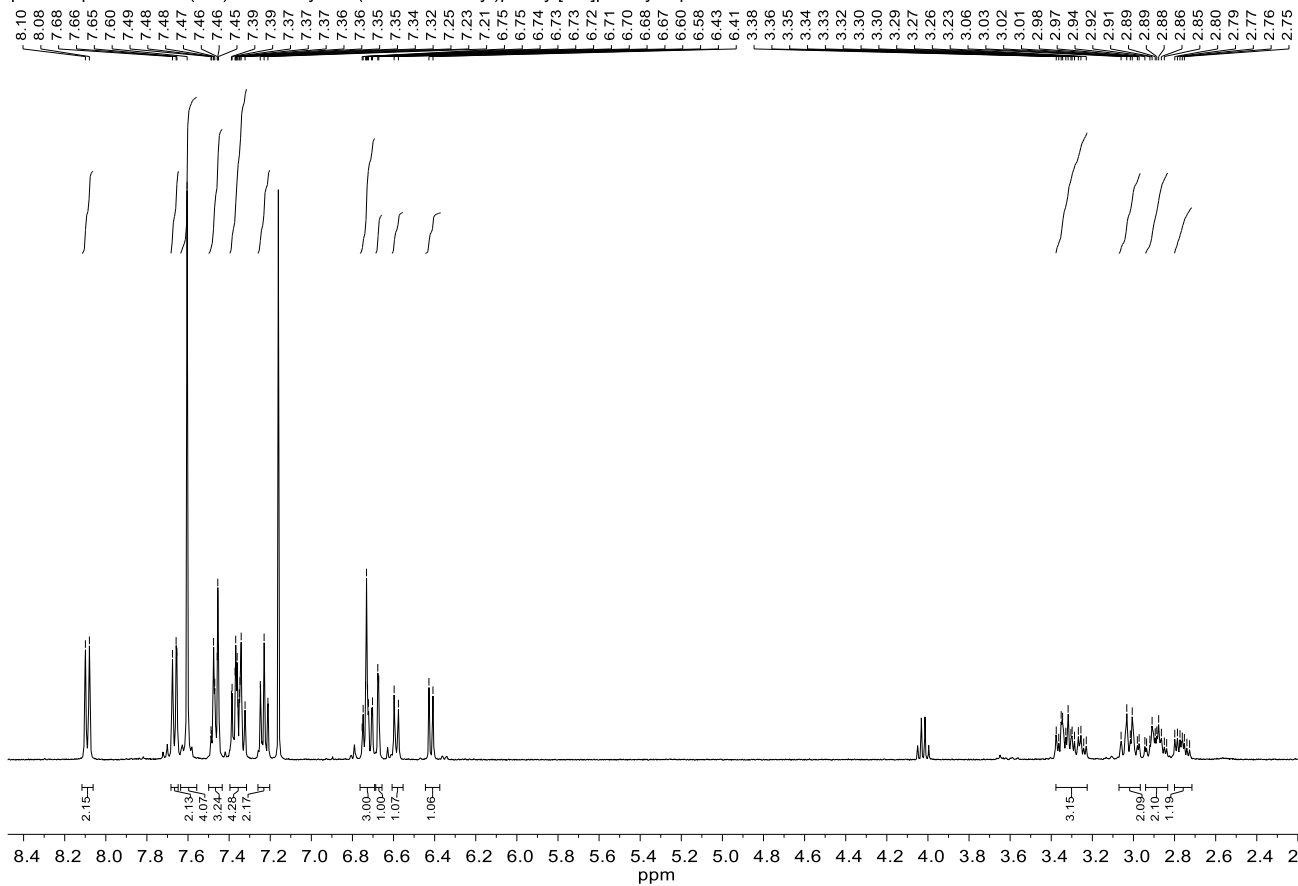


(rac, "trans") 4-Benzoyl-16-(4'-N-carbazolyl)phenyl[2.2]paracyclophane (8):

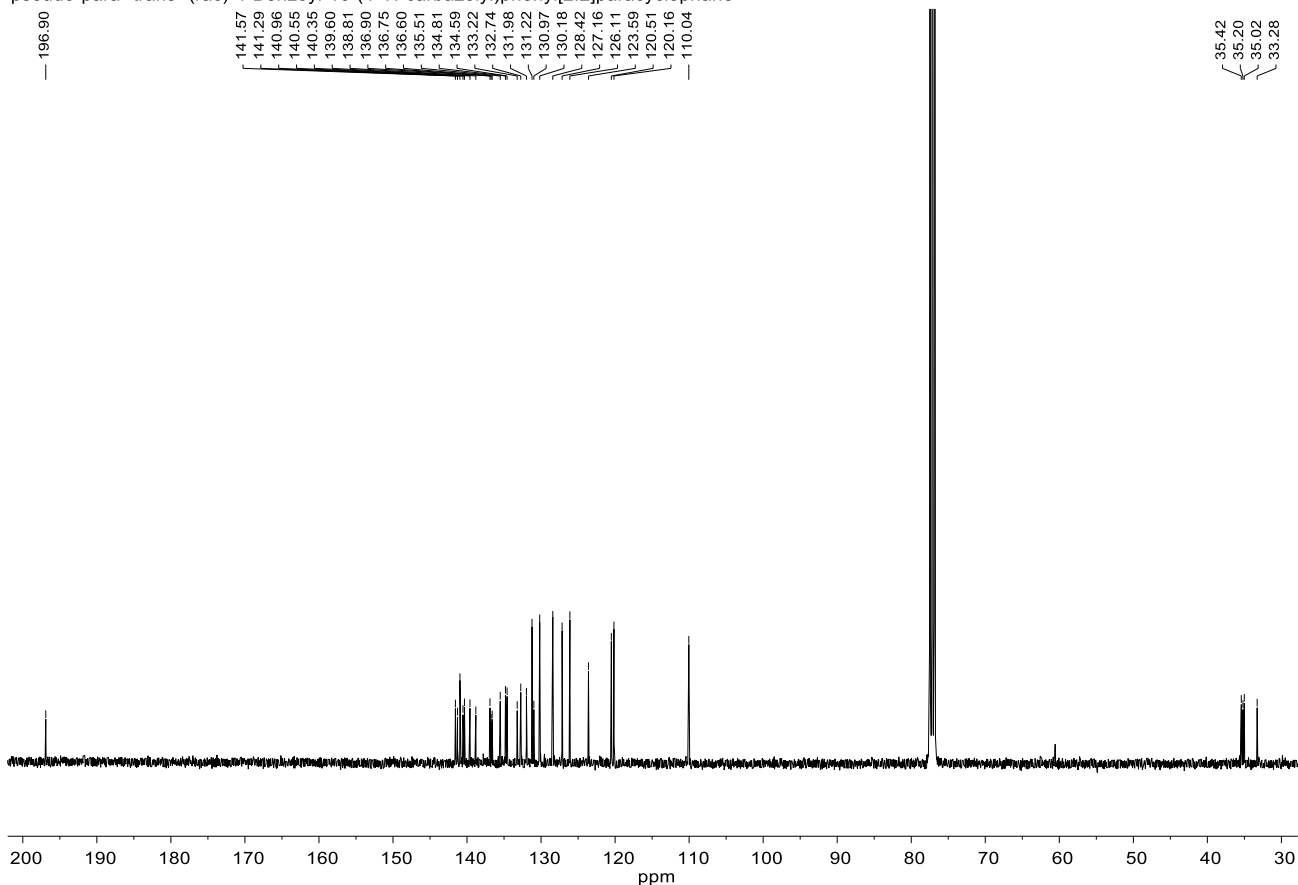
In a pressure vial were charged (*rac*)-4-bromo-16-benzoyl[2.2]paracyclophane (**6**) (97.8 mg, 250  $\mu$ mol, 1.00 equiv.), 4-(*N*-carbazolyl)phenyl boronic acid (144 mg, 500  $\mu$ mol, 2.00 equiv.), Cs<sub>2</sub>CO<sub>3</sub> (244 mg, 750  $\mu$ mol, 3.00 equiv.), and Pd(PPh<sub>3</sub>)<sub>2</sub>Cl<sub>2</sub> (21.1 mg, 30.0  $\mu$ mol, 10 mol%). The sealed vial was evacuated and flushed with argon three times. Through the septum 6 mL of degassed tetrahydrofuran and 1.5 mL of degassed water were added, then heated to 75 °C and stirred for 16 h. The reaction mixture was diluted in 50 mL of ethyl acetate and washed first with sat. aqueous NH<sub>4</sub>Cl solution (3  $\times$  30 mL) and then with brine (30 mL). The organic layer was dried over Na<sub>2</sub>SO<sub>4</sub> and the solvent was removed under reduced pressure. The crude product was purified by column chromatography (silica gel, cyclohexane/ethyl acetate; 50/1) to yield 106 mg of the product as a white solid (191  $\mu$ mol, 76%).

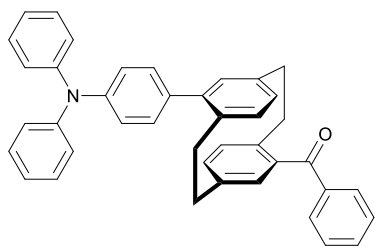
$R_f$  = 0.14 (CH/EA 50:1). – <sup>1</sup>H NMR (400 MHz, CDCl<sub>3</sub>)  $\delta$  = 8.09 (d,  $J$  = 7.8 Hz, 2H), 7.70 – 7.64 (m, 2H), 7.60 (s, 4H), 7.49 – 7.45 (m, 3H), 7.41 – 7.31 (m, 4H), 7.25 – 7.21 (m, 2H), 6.77 – 6.69 (m, 3H), 6.67 (d,  $J$  = 1.9 Hz, 1H), 6.59 (d,  $J$  = 8.3 Hz, 1H), 6.42 (d,  $J$  = 7.8 Hz, 1H), 3.44 – 3.18 (m, 3H), 3.06 – 2.97 (m, 2H), 2.96 – 2.83 (m, 2H), 2.76 (ddd,  $J$  = 14.3, 10.2, 5.2 Hz, 1H) ppm. – <sup>13</sup>C NMR (101 MHz, CDCl<sub>3</sub>)  $\delta$  = 196.90 (C<sub>quat.</sub>, CO), 141.57 (C<sub>quat.</sub>), 141.29 (C<sub>quat.</sub>), 140.96 (C<sub>quat.</sub>), 140.55 (C<sub>quat.</sub>), 140.35 (C<sub>quat.</sub>), 139.60 (C<sub>quat.</sub>), 138.81 (C<sub>quat.</sub>), 136.90 (C<sub>quat.</sub>), 136.75 (C<sub>quat.</sub>), 136.60 (C<sub>quat.</sub>), 135.51 (+), 134.81 (+), 134.59 (+), 133.22 (+), 132.74 (+), 131.98 (+), 131.22 (+), 130.97 (+), 130.18 (+), 128.42 (+), 127.16 (+), 126.11(+), 123.59 (C<sub>quat.</sub>), 120.51 (+), 120.16 (+), 110.04 (+), 35.42 (–), 35.20 (–), 35.02 (–), 33.28 (–) ppm. – Mp : 145-150 °C. – IR (ATR):  $\tilde{\nu}$  = 3045 (vw), 2922 (vw), 2852 (vw), 1651 (w), 1596 (vw), 1514 (w), 1478 (vw), 1449 (w), 1335 (vw), 1315 (vw), 1269 (w), 1228 (w), 1171 (vw), 1026 (vw), 913 (vw), 838 (vw), 748 (w), 723 (w), 701 (w), 656 (vw), 565 (vw), 489 (vw), 423 (vw) cm<sup>-1</sup>. – MS (FAB, 3-NBA),  $m/z$ : 554 [M+H]<sup>+</sup>, 553 [M]<sup>+</sup>. – HRMS (C<sub>41</sub>H<sub>31</sub>NO) calc.: 553.2406; found: 553.2403.

pseudo-para "trans" (rac)-4-Benzoyl-16-(4'-N-carbazolyl)phenyl[2.2]paracyclophane



pseudo-para "trans" (rac)-4-Benzoyl-16-(4'-N-carbazolyl)phenyl[2.2]paracyclophane

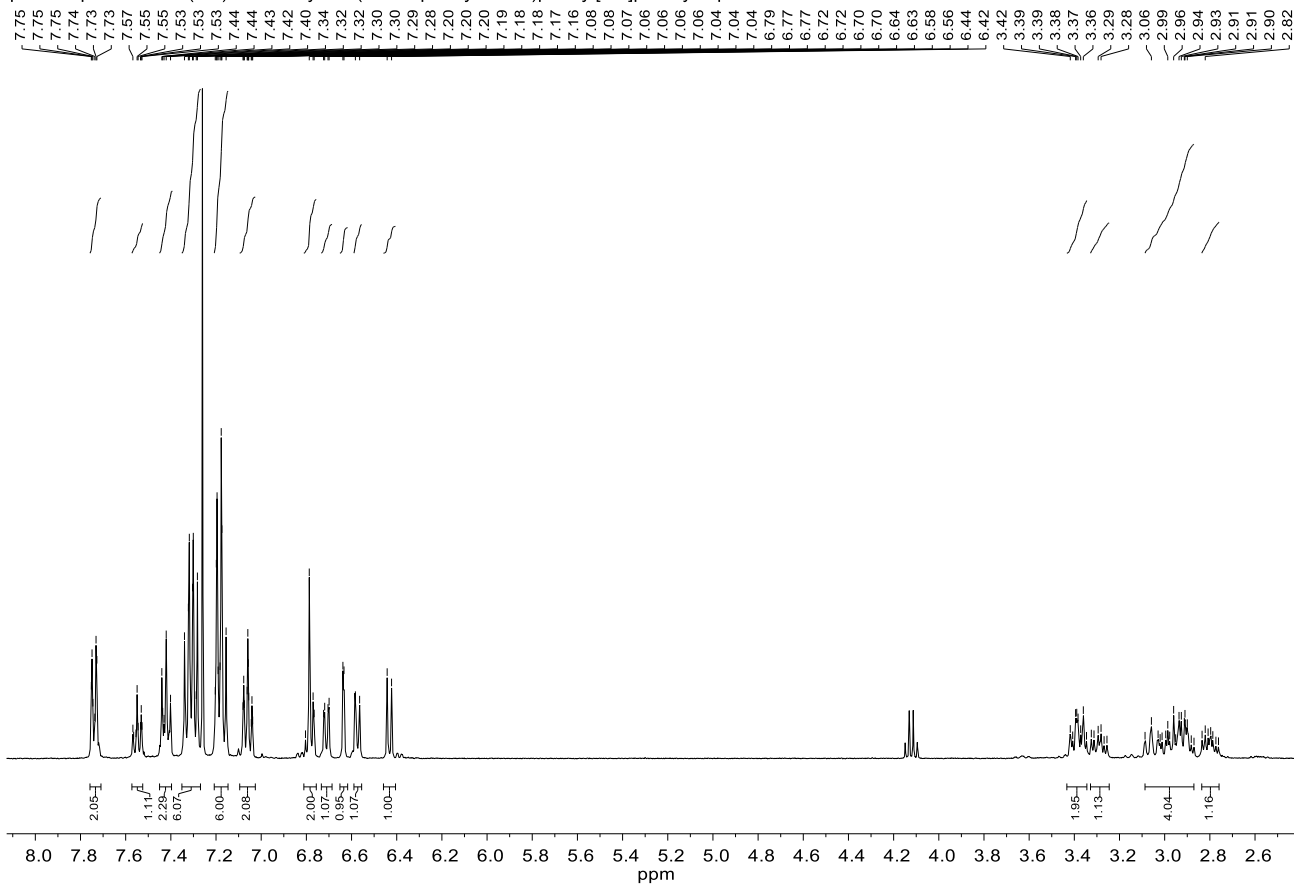


(rac, "trans") 4-Benzoyl-16-(4'-N-diphenylamino)phenyl[2.2]paracyclophane (7):

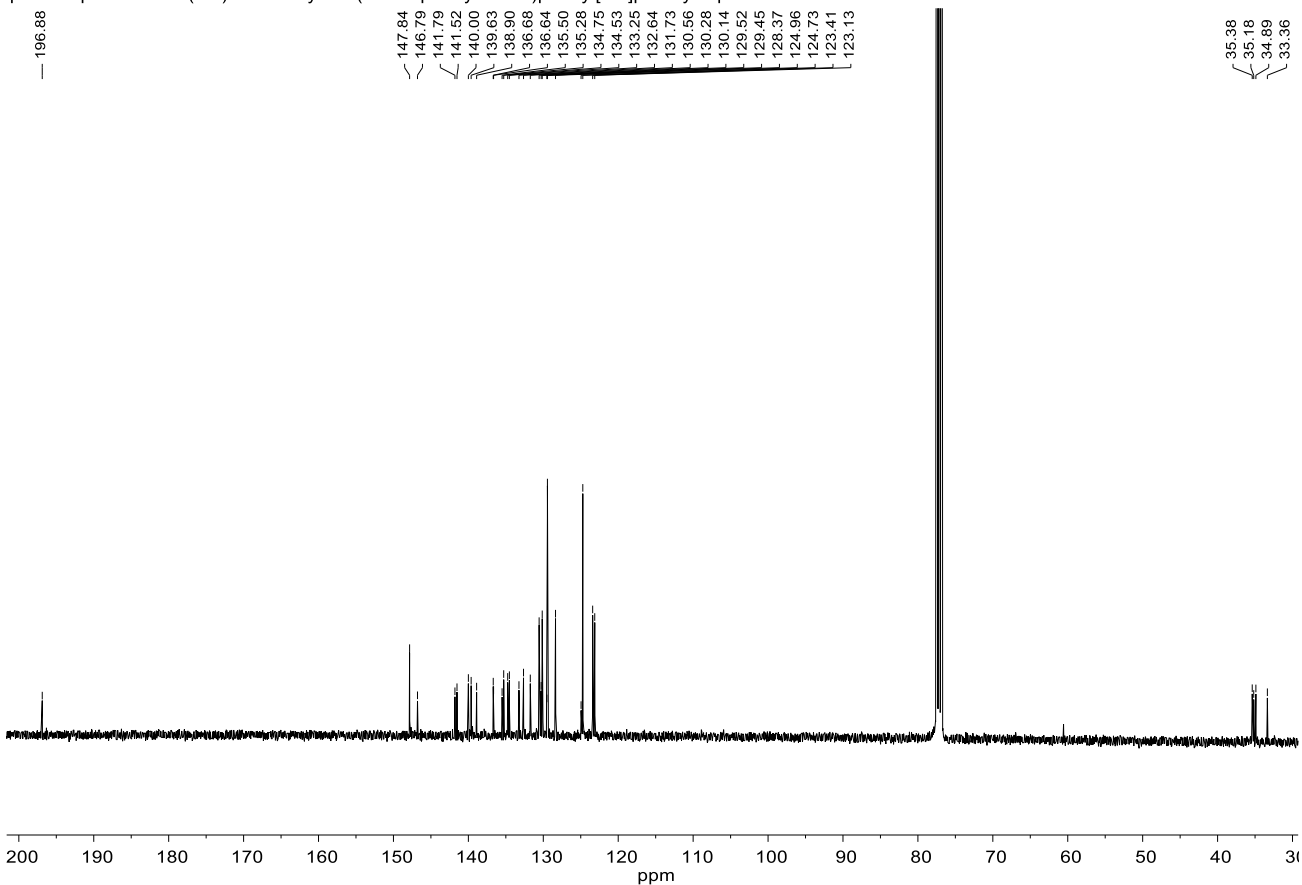
In a pressure vial were charged (*rac*)-4-bromo-16-benzoyl[2.2]paracyclophane (**6**) (97.8 mg, 250  $\mu$ mol, 1.00 equiv.), 4-(*N*-diphenylamino)phenyl boronic acid (144 mg, 500  $\mu$ mol, 2.00 equiv.), Cs<sub>2</sub>CO<sub>3</sub> (244 mg, 750  $\mu$ mol, 3.00 equiv.), and Pd(PPh<sub>3</sub>)<sub>2</sub>Cl<sub>2</sub> (21.1 mg, 30.0  $\mu$ mol, 10 mol%). The sealed vial was evacuated and flushed with argon three times. Through the septum 6 mL of degassed tetrahydrofuran and 1.5 mL of degassed water were added, then heated to 75 °C and stirred for 16 h. The reaction mixture was diluted in 50 mL of ethyl acetate and washed first with sat. aqueous NH<sub>4</sub>Cl solution (3  $\times$  30 mL) and then with brine (30 mL). The organic layer was dried over Na<sub>2</sub>SO<sub>4</sub> and the solvent was removed under reduced pressure. The crude product was purified by column chromatography (silica gel, cyclohexane/ethyl acetate; 50/1) to yield 92.2 mg of the product as an off-white solid (65%, 166  $\mu$ mol).

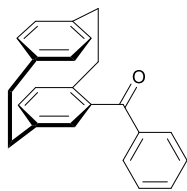
$R_f = 0.14$  (CH/EA 50:1). – <sup>1</sup>H NMR (400 MHz, CDCl<sub>3</sub>)  $\delta = 7.79 - 7.69$  (m, 2H), 7.59 – 7.51 (m, 1H), 7.42 (t,  $J = 7.7$  Hz, 2H), 7.35 – 7.27 (m, 6H), 7.21 – 7.14 (m, 6H), 7.10 – 7.02 (m, 2H), 6.81 – 6.75 (m, 2H), 6.71 (dd,  $J = 7.8, 1.9$  Hz, 1H), 6.64 (d,  $J = 1.9$  Hz, 1H), 6.57 (d,  $J = 7.5$  Hz, 1H), 6.43 (d,  $J = 7.8$  Hz, 1H), 3.44 – 3.34 (m, 2H), 3.34 – 3.24 (m, 1H), 3.11 – 2.86 (m, 4H), 2.85 – 2.74 (m, 1H) ppm. – <sup>13</sup>C NMR (101 MHz, CDCl<sub>3</sub>)  $\delta = 196.88$  (C<sub>quat.</sub>, CO), 147.84 (C<sub>quat.</sub>), 146.79 (C<sub>quat.</sub>), 141.79 (C<sub>quat.</sub>), 141.52 (C<sub>quat.</sub>), 140.00 (C<sub>quat.</sub>), 139.63 (C<sub>quat.</sub>), 138.90 (C<sub>quat.</sub>), 136.68 (C<sub>quat.</sub>), 136.64 (C<sub>quat.</sub>), 135.50 (C<sub>quat.</sub>), 135.28 (+), 134.75 (+), 134.53 (+), 133.25 (+), 132.64 (+), 131.73 (+), 130.56 (+), 130.28 (+), 130.14 (+), 129.52 (+), 129.45 (+), 128.37 (+), 124.96 (+), 124.73 (+), 123.41 (+), 123.13 (+), 35.38 (–), 35.18 (–), 34.89 (–), 33.36 (–) ppm. – Mp : 125-130 °C. – IR (ATR):  $\tilde{\nu} = 3058$  (vw), 3032 (vw), 2923 (w), 2853 (vw), 2258 (vw), 1715 (vw), 1652 (w), 1589 (w), 1487 (w), 1447 (vw), 1270 (m), 1151 (w), 1110 (w), 1024 (m), 819 (w), 753 (w), 695 (m), 617 (w), 510 (w), 483 (w), 426 (vw) cm<sup>-1</sup>. – MS (FAB, 3-NBA),  $m/z$ : 556 [M+H]<sup>+</sup>, 555 [M]<sup>+</sup>. – HRMS (C<sub>41</sub>H<sub>33</sub>NO) calc.: 555.2562; found: 555.2564.

## pseudo-para "trans" (rac)-4-Benzoyl-16-(4'-N-diphenylamino)phenyl[2.2]paracyclophane



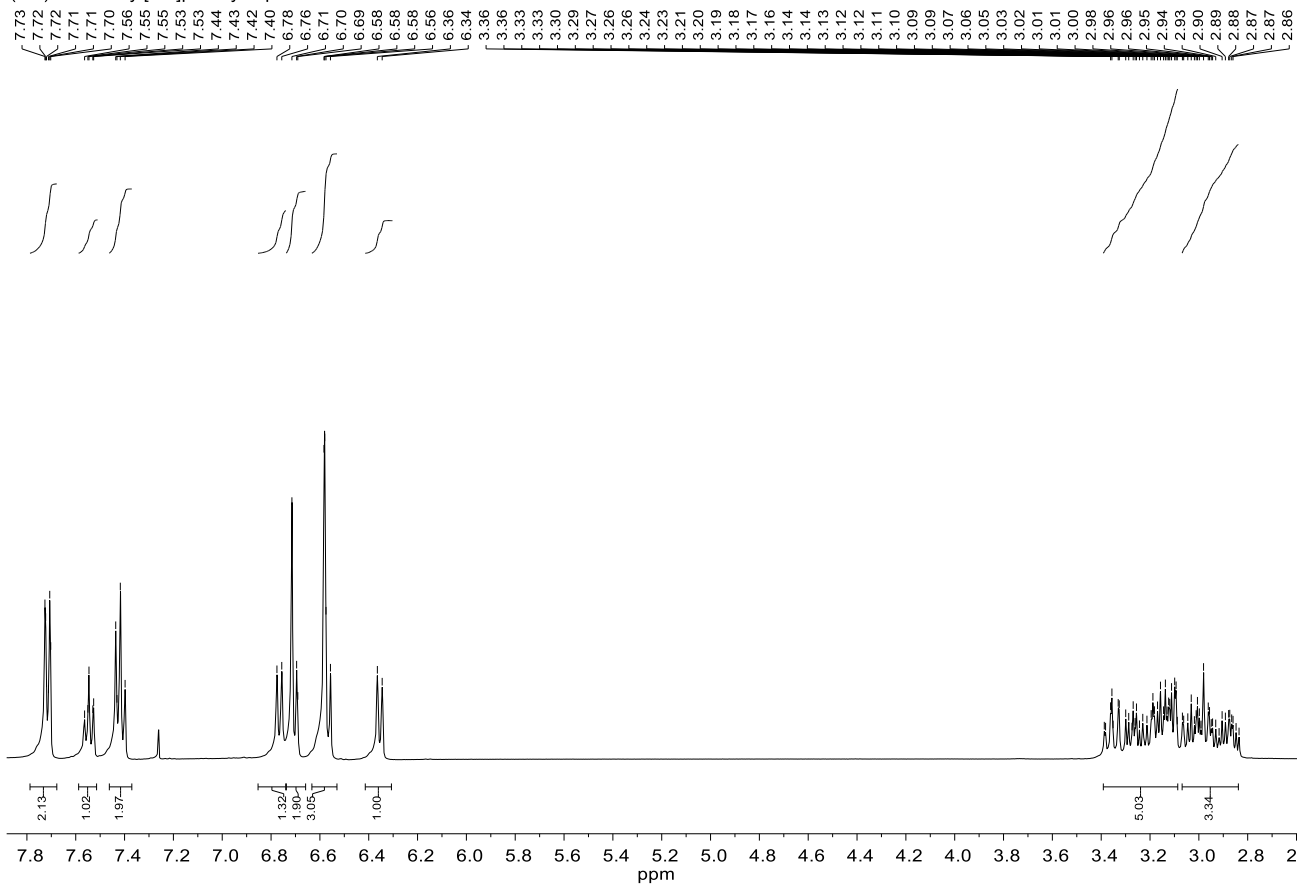
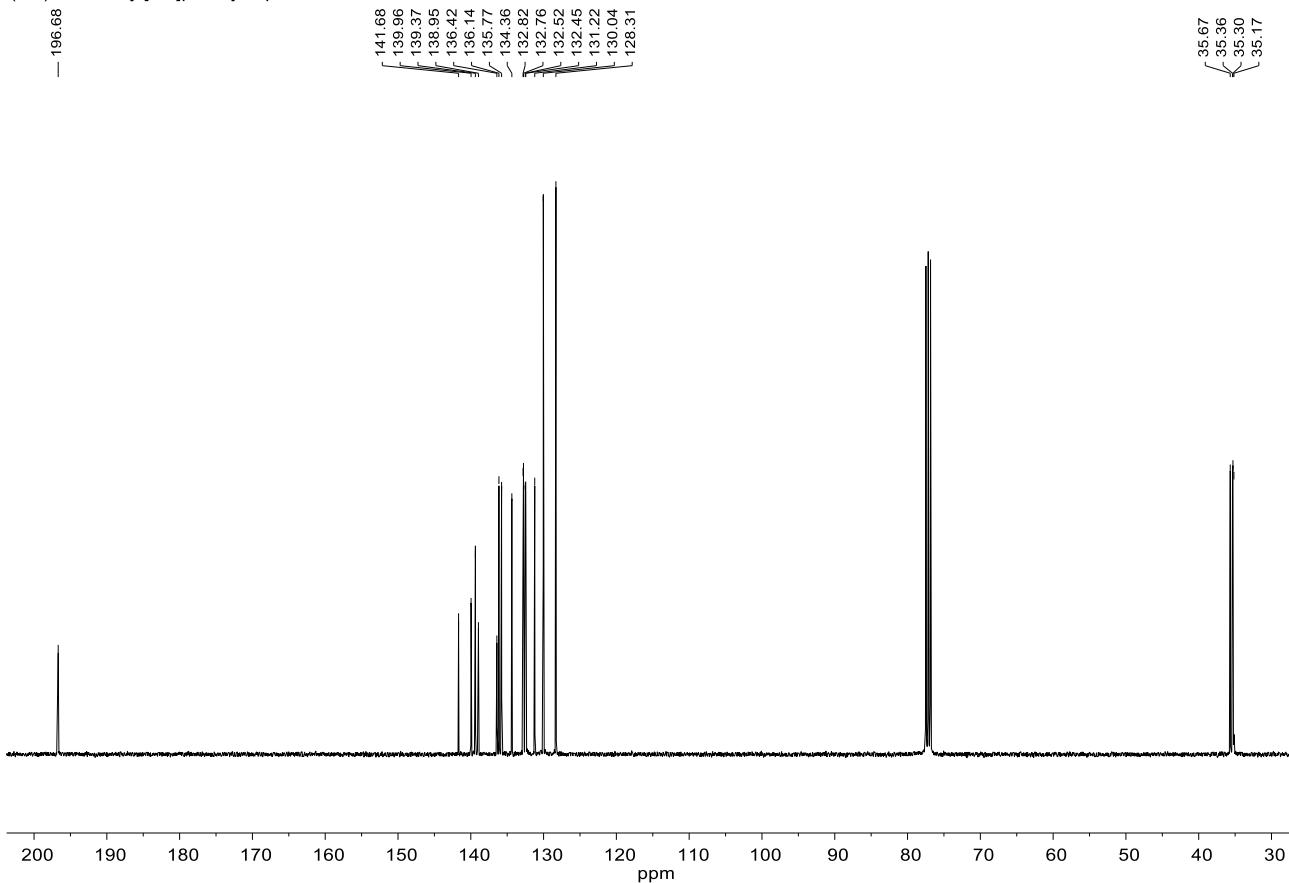
## pseudo-para "trans" (rac)-4-Benzoyl-16-(4'-N-diphenylamino)phenyl[2.2]paracyclophane

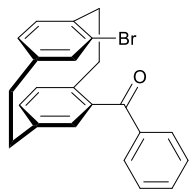


(rac)-4-Benzoyl[2.2]paracyclophane (1)

In a 250 mL flask, [2.2]paracyclophane (10.4 g, 50.0 mmol, 1.00 equiv.) was dissolved in 100 mL of dichloromethane and cooled to  $-10\text{ }^{\circ}\text{C}$ . A solution of benzoyl chloride (11.5 mL, 14.1 g, 100 mmol, 2.00 equiv.) and  $\text{AlCl}_3$  (11.7 g, 88.0 mmol, 1.75 equiv.) in 50 mL of dichloromethane were added and stirred for 1 h. The reaction mixture was filtered through glass wool and hydrolyzed with ice. Extraction was carried out with dichloromethane (200 mL), afterwards the organic layer was washed with aqueous  $\text{NaHCO}_3$  (200 mL) solution and brine (200 mL), then dried over  $\text{Na}_2\text{SO}_4$ . The solvent was evaporated under reduced pressure and the residue was recrystallized in ethanol to yield 12.4 g (39.7 mmol, 79%) of colorless crystals.

$R_f = 0.53$  (CH/EA 40:1) –  $^1\text{H NMR}$  (400 MHz,  $\text{CDCl}_3$ )  $\delta = 7.72$  (d,  $J = 7.8$  Hz, 2H), 7.56 – 7.53 (m, 1H), 7.42 (t,  $J = 7.7$  Hz, 2H), 6.77 (d,  $J = 7.9$  Hz, 1H), 6.71 – 6.69 (m, 2H), 6.58 – 6.55 (m, 3H), 6.35 (d,  $J = 7.9$  Hz, 1H), 3.39 – 3.09 (m, 5H), 3.07 – 2.84 (m, 3H) ppm. –  $^{13}\text{C NMR}$  (101 MHz,  $\text{CDCl}_3$ )  $\delta = 196.68$  ( $\text{C}_{\text{quat}}$ , CO), 141.68 ( $\text{C}_{\text{quat}}$ ), 139.96 ( $\text{C}_{\text{quat}}$ ), 139.37 ( $\text{C}_{\text{quat}}$ ), 138.95 ( $\text{C}_{\text{quat}}$ ), 136.42 ( $\text{C}_{\text{quat}}$ ), 136.14 (+), 135.77 (+), 134.36 (+), 132.82 (+), 132.76 (+), 132.52 (+), 132.45 (+), 131.22 (+), 130.04 (+), 128.31 (+), 35.67 (–), 35.36 (–), 35.30 (–), 35.17 (–) ppm. – IR (ATR)  $\tilde{\nu} = 2919$  (w), 2848 (vw), 1649 (m), 1594 (w), 1446 (w), 1411 (vw), 1318 (w), 1294 (w), 1269 (w), 1196 (w), 976 (w), 941 (w), 907 (w), 891 (w), 835 (w), 803 (w), 726 (w), 700 (m), 656 (w), 634 (m), 509 (m), 454 (vw)  $\text{cm}^{-1}$ . – MS (EI, 70 eV)  $m/z$  [%] = 313 (25)  $[\text{M}+\text{H}]^+$ , 312 (100)  $[\text{M}]^+$ , 208 (86)  $[\text{M}-\text{C}_8\text{H}_8]^+$ , 207 (73)  $[\text{M}-\text{C}_8\text{H}_9]^+$ , 105 (11)  $[\text{C}_8\text{H}_9]^+$ , 104 (29)  $[\text{C}_8\text{H}_8]^+$ . – HRMS ( $\text{C}_{23}\text{H}_{20}\text{O}$ ) calc. 312.1509; found 312.1510. The analytical data matches that of the literature.<sup>7</sup>

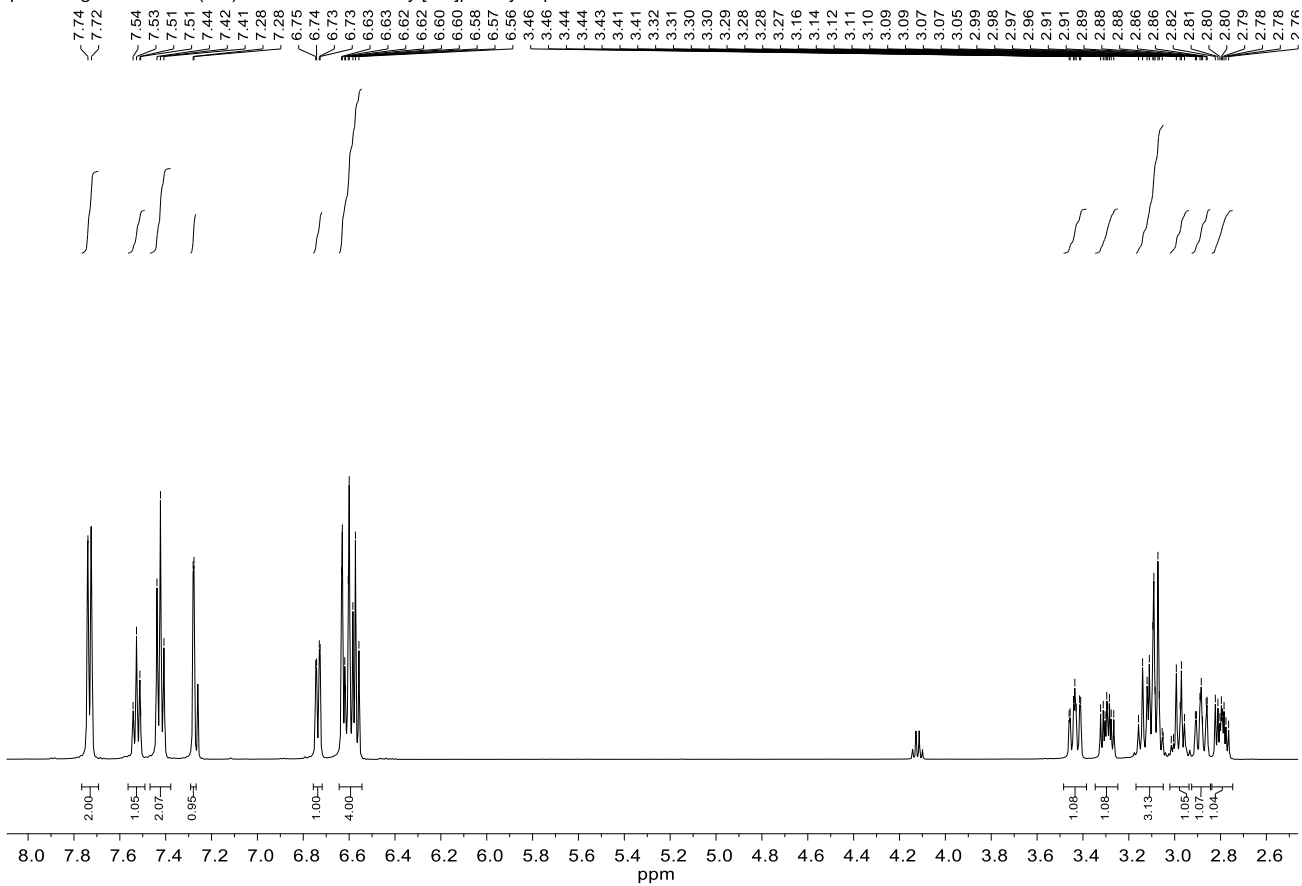
**(rac)-4-Benzoyl[2.2]paracyclophane****(rac)-4-Benzoyl[2.2]paracyclophane**

(rac, “cis”)-4-Bromo-13-benzoyl[2.2]paracyclophane (2)

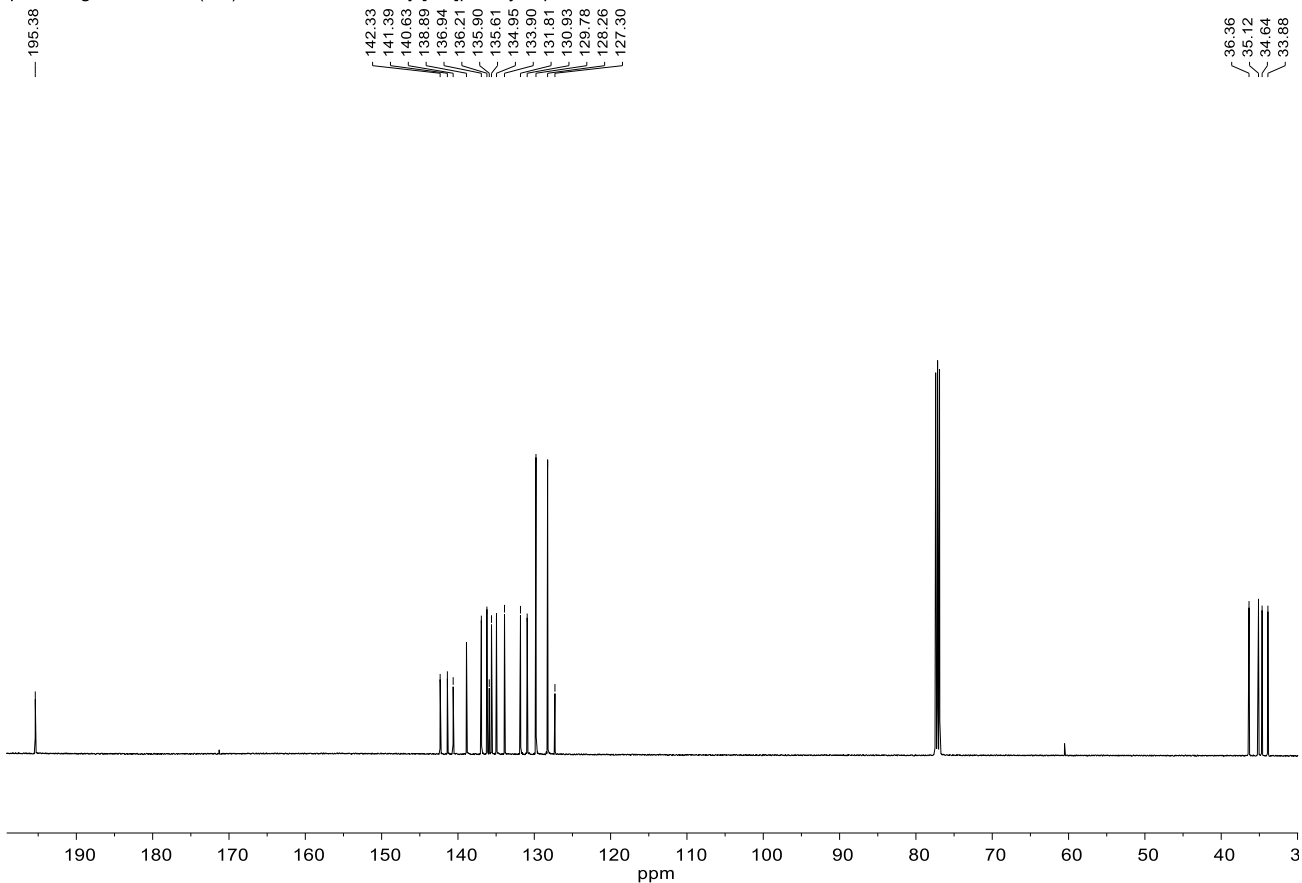
A solution of 2.51 mL bromine (7.82 g, 49.0 mmol, 1.02 equiv.) in 60 mL of dichloromethane was prepared in a dropping funnel and 5 mL of this solution were added to iron filings (50.0 mg, 960  $\mu\text{mol}$ , 2 mol%) in a 500 mL three neck flask and stirred for 1 h at room temperature. Then 100 mL of dichloromethane and (*rac*)-4-benzoyl[2.2]paracyclophane (**1**) (15.0 g, 48.0 mmol, 1.00 equiv.) were added and stirred for another 30 min. The remainder of the bromine solution was added dropwise over a period of 5 h and the mixture was stirred for 3 days. The reaction was quenched with a saturated sodium sulfite solution (200 mL) and stirred for 30 min until full discoloration of the mixture. The organic phase was separated, washed with brine (200 mL) and dried over  $\text{Na}_2\text{SO}_4$ . The filtrate was evaporated and the residue was purified by flash chromatography (silica, 40:1 cyclohexane:ethyl acetate) to yield 8.60 g (21.9 mmol, 46%) of a white solid.

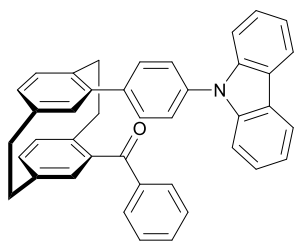
$R_f = 0.23$  (CH/EA 40:1) –  $^1\text{H NMR}$  (500 MHz,  $\text{CDCl}_3$ )  $\delta = 7.73$  (d,  $J = 7.7$  Hz, 2H), 7.53 (t,  $J = 7.4$  Hz, 1H), 7.42 (t,  $J = 7.6$  Hz, 2H), 7.28 (d,  $J = 1.9$  Hz, 1H), 6.74 (dd,  $J = 7.7, 1.9$  Hz, 1H), 6.68 – 6.53 (m, 4H), 3.44 (ddd,  $J = 12.8, 9.6, 2.3$  Hz, 1H), 3.29 (ddd,  $J = 13.2, 9.6, 5.7$  Hz, 1H), 3.18 – 3.04 (m, 3H), 3.02 – 2.94 (m, 1H), 2.88 (ddd,  $J = 12.9, 10.0, 2.3$  Hz, 1H), 2.79 (ddd,  $J = 13.2, 10.0, 5.7$  Hz, 1H) ppm –  $^{13}\text{C NMR}$  (126 MHz,  $\text{CDCl}_3$ )  $\delta = 195.38$  ( $\text{C}_{\text{quat}}$ , CO), 142.33 ( $\text{C}_{\text{quat}}$ ), 141.39 ( $\text{C}_{\text{quat}}$ ), 140.63 ( $\text{C}_{\text{quat}}$ ), 138.89 ( $\text{C}_{\text{quat}}$ ), 136.94 (+), 136.21 (+), 135.90 ( $\text{C}_{\text{quat}}$ ), 135.61 (+), 134.95 (+), 133.90 (+), 131.81 (+), 130.93 (+), 129.78 (+), 128.26 (+), 127.30 ( $\text{C}_{\text{quat}}$ ), 36.36 (–), 35.12 (–), 34.64 (–), 33.88 (–) ppm. – IR (ATR)  $\tilde{\nu} = 2927$  (w), 1742 (w), 1649 (m), 1587 (w), 1471 (w), 1445 (w), 1388 (w), 1268 (m), 1240 (w), 1205 (w), 1030 (w), 981 (w), 951 (w), 890 (w), 836 (w), 800 (w), 735 (m), 700 (m), 652 (w), 637 (w), 604 (w), 519 (w), 479 (w), 390 (vw)  $\text{cm}^{-1}$ . – MS (EI, 70 eV)  $m/z$  [%] = 393 (12)  $[\text{M}(^{81}\text{Br})+\text{H}]^+$ , 392 (50)  $[\text{M}(^{81}\text{Br})]^+$ , 391 (12)  $[\text{M}(^{79}\text{Br})+\text{H}]^+$ , 390 (47)  $[\text{M}(^{79}\text{Br})]^+$ , 208 (100)  $[\text{M}-\text{C}_8\text{H}_7\text{Br}]^+$ , 207 (91)  $[\text{M}-\text{C}_8\text{H}_8\text{Br}]^+$ , 106 (39)  $[\text{CHOPh}]^+$ . – HRMS ( $\text{C}_{23}\text{H}_{19}^{79}\text{BrO}$ ) calc. 390.0614; found 390.0612.

## pseudo-geminal "cis" (rac)-4-Bromo-13-benzoyl[2.2]paracyclophane



## pseudo-geminal "cis" (rac)-4-Bromo-13-benzoyl[2.2]paracyclophane



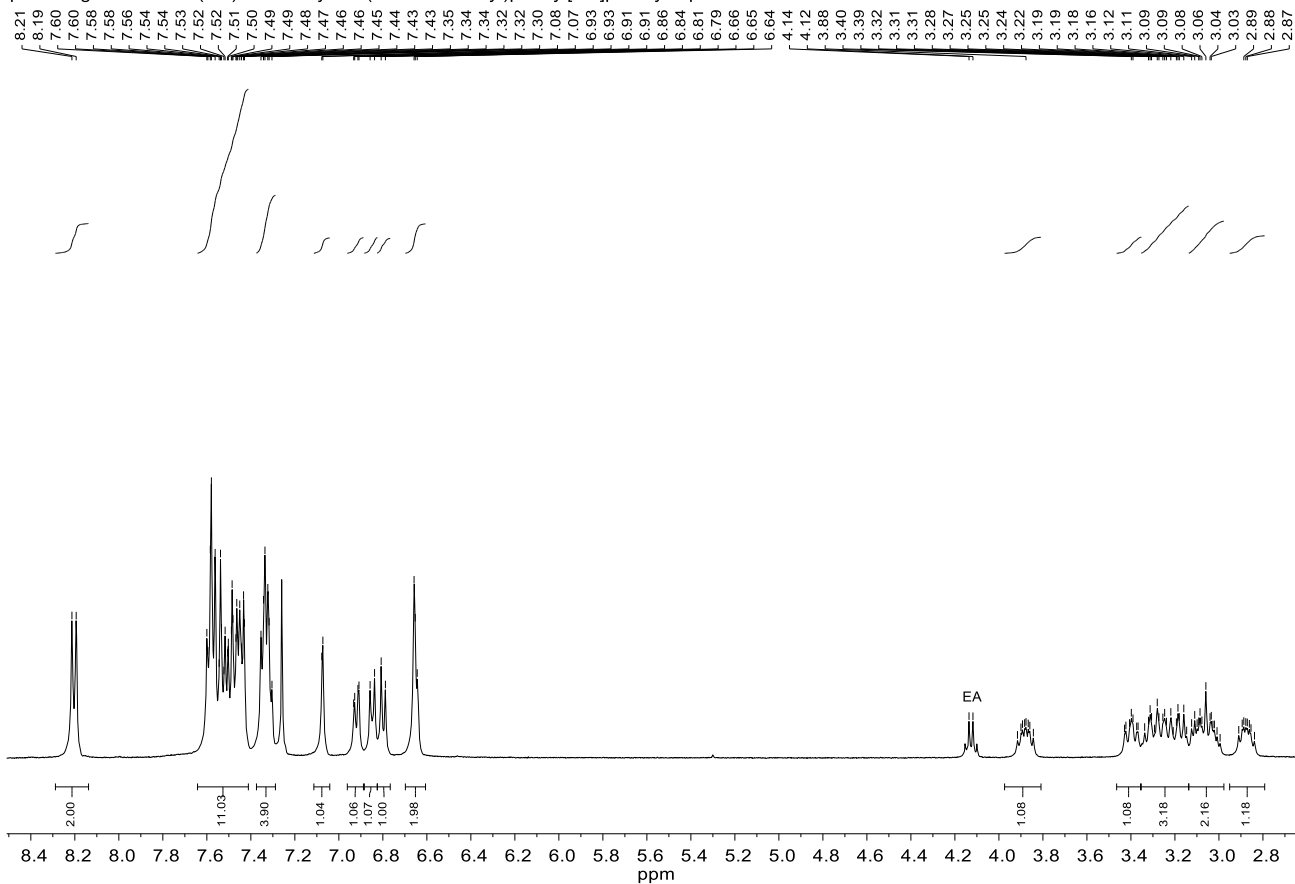
(rac, "cis") 4-Benzoyl-13-(4'-N-carbazolyl)phenyl[2.2]paracyclophane (4):

In a pressure vial were charged with (*rac*)-4-bromo-13-benzoyl[2.2]paracyclophane (**2**) (156.5 mg, 400  $\mu$ mol, 1.00 equiv.), 4-(*N*-carbazolyl)phenyl boronic acid (229 mg, 800  $\mu$ mol, 2.00 equiv.),  $K_3PO_4$  (170 mg, 800  $\mu$ mol, 2.00 equiv.),  $Pd(OAc)_2$  (8.98 mg, 40.0  $\mu$ mol, 10 mol%) and 2-dicyclohexylphosphino-2,6-diisopropoxybiphenyl ("RuPhos") (37.3 mg, 80.0  $\mu$ mol, 20 mol%). The sealed vial was evacuated and flushed

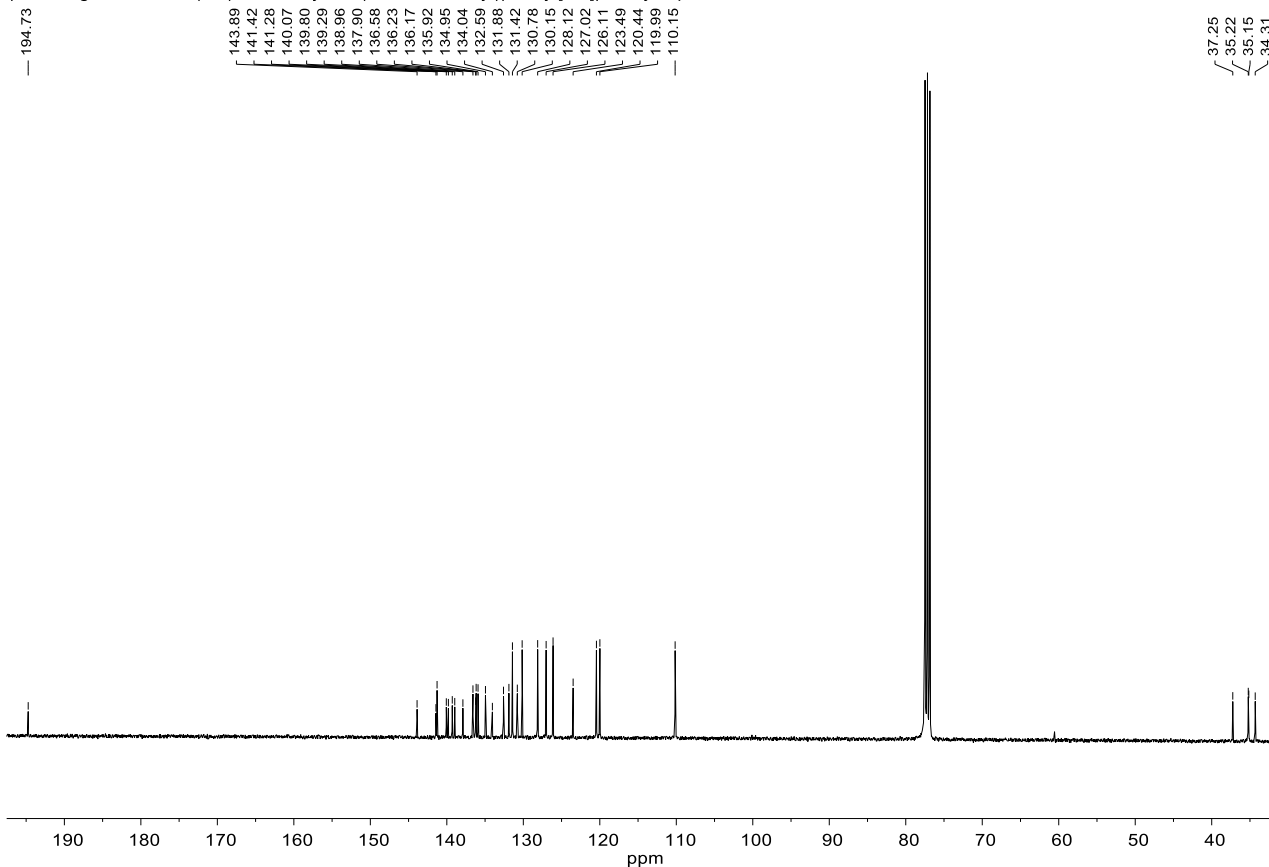
with argon three times. Through the septum 7 mL of degassed toluene and 1 mL of degassed water were added, then heated to 75  $^{\circ}C$  and stirred for 16 h. The reaction mixture was diluted in 50 mL of ethyl acetate and washed first with sat. aqueous  $NH_4Cl$  solution (3  $\times$  30 mL) and then with brine (30 mL). The organic layer was dried over  $Na_2SO_4$  and the solvent was removed under reduced pressure. The crude product was purified by column chromatography (silica gel, cyclohexane/ethyl acetate; 20/1) to yield 126 mg of the product as a white solid (227  $\mu$ mol, 57%).

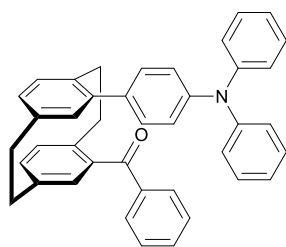
$R_f = 0.34$  (CH/EA 20:1). –  $^1H$  NMR (400 MHz,  $CDCl_3$ )  $\delta = 8.20$  (d,  $J = 7.8$  Hz, 2H), 7.64 – 7.40 (m, 11H), 7.33 (td,  $J = 7.4, 4.9$  Hz, 4H), 7.08 (d,  $J = 2.0$  Hz, 1H), 6.92 (dd,  $J = 7.8, 1.9$  Hz, 1H), 6.85 (d,  $J = 8.1$  Hz, 1H), 6.80 (d,  $J = 7.7$  Hz, 1H), 6.66 (d,  $J = 2.1$  Hz, 2H), 3.88 (ddd,  $J = 13.4, 9.3, 6.4$  Hz, 1H), 3.40 (ddd,  $J = 12.3, 9.2, 2.5$  Hz, 1H), 3.35 – 3.14 (m, 3H), 3.14 – 2.95 (m, 2H), 2.87 (ddd,  $J = 13.0, 9.2, 6.3$  Hz, 1H) ppm. –  $^{13}C$  NMR (101 MHz,  $CDCl_3$ )  $\delta = 194.73$  ( $C_{quat.}$ , CO), 143.89 ( $C_{quat.}$ ), 141.42 ( $C_{quat.}$ ), 141.28 ( $C_{quat.}$ ), 140.07 ( $C_{quat.}$ ), 139.80 ( $C_{quat.}$ ), 139.29 ( $C_{quat.}$ ), 138.96 ( $C_{quat.}$ ), 137.90 ( $C_{quat.}$ ), 136.58 (+), 136.23 ( $C_{quat.}$ ), 136.17 (+), 135.92 (+), 134.95 (+), 134.04 ( $C_{quat.}$ ), 132.59 (+), 131.88 (+), 131.42 (+), 130.78 (+), 130.15 (+), 128.12 (+), 127.02 (+), 126.11 (+), 123.49 ( $C_{quat.}$ ), 120.44 (+), 119.99 (+), 110.15 (+), 37.25 (–), 35.22 (–), 35.15 (–), 34.31 (–) ppm. – Mp : 165-175  $^{\circ}C$ . – IR (ATR):  $\tilde{\nu} = 2922$  (vw), 1733 (vw), 1650 (vw), 1595 (vw), 1515 (vw), 1477 (vw), 1450 (w), 1334 (vw), 1315 (vw), 1269 (vw), 1230 (w), 978 (vw), 914 (vw), 837 (vw), 749 (vw), 723 (w), 700 (w), 632 (vw), 566 (vw), 525 (vw), 487 (vw), 424 (vw)  $cm^{-1}$  – MS (FAB, 3-NBA),  $m/z$ : 554  $[M+H]^+$ , 553  $[M]^+$ . – HRMS ( $C_{41}H_{31}NO$ ) calc.: 553.2406; found: 553.2405.

pseudo-geminal "cis" (rac)-4-Benzoyl-13-(4'-N-carbazoyl)phenyl[2.2]paracyclophane



pseudo-geminal "cis" (rac)-4-Benzoyl-13-(4'-N-carbazoyl)phenyl[2.2]paracyclophane



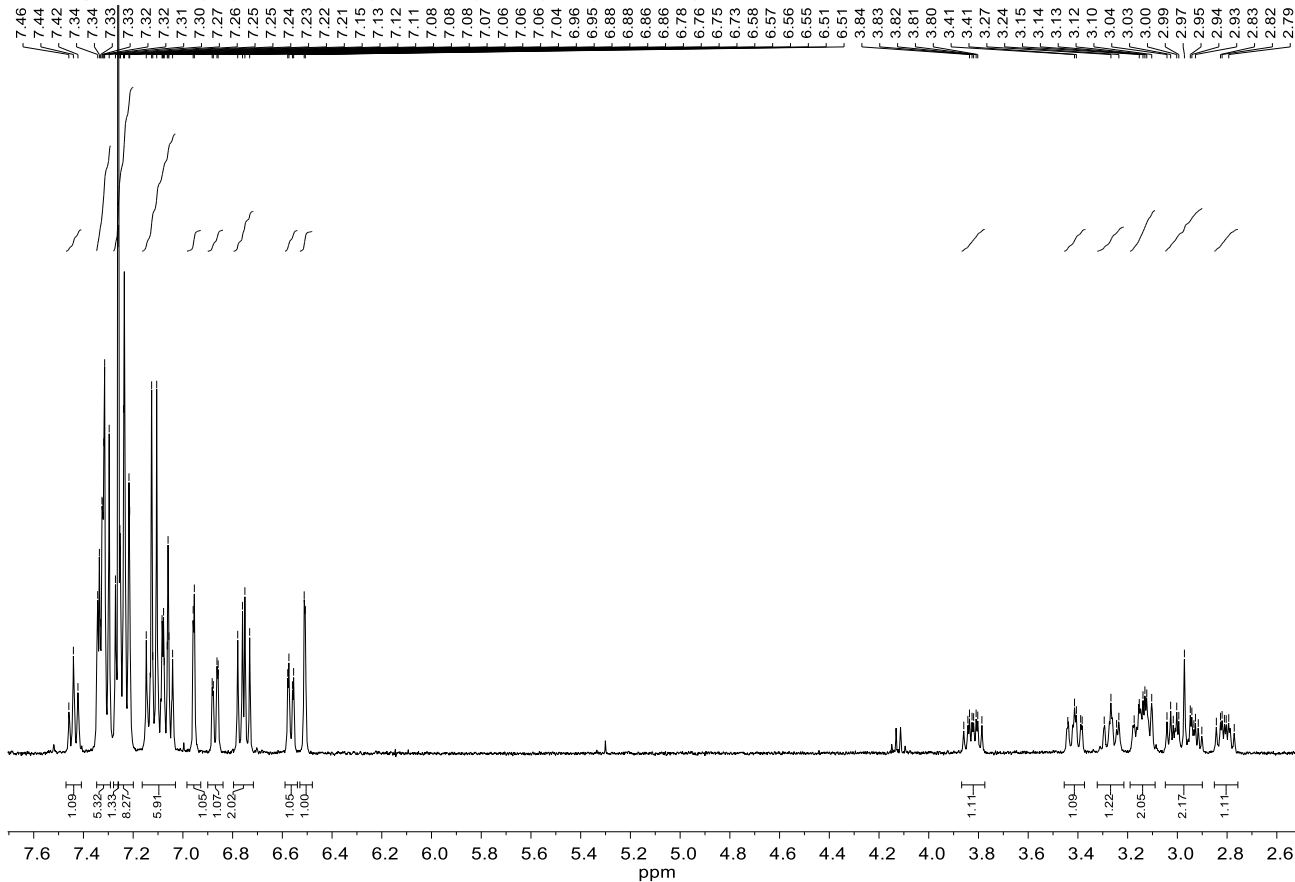
(rac, "cis") 4-Benzoyl-13-(4'-N-diphenylamino)phenyl[2.2]paracyclophane (3):

In a pressure vial were charged with (*rac*)-4-bromo-13-benzoyl[2.2]paracyclophane (**2**) (156.5 mg, 400  $\mu$ mol, 1.00 equiv.), 4-(*N*-diphenylamino)phenyl boronic acid (231 mg, 800  $\mu$ mol, 2.00 equiv.),  $K_3PO_4$  (170 mg, 800  $\mu$ mol, 2.00 equiv.),  $Pd(OAc)_2$  (4.50 mg, 20.0  $\mu$ mol, 5 mol%) and 2-dicyclohexylphosphino-2,6-diisopropoxybiphenyl ("RuPhos") (18.7 mg, 40.0  $\mu$ mol, 10 mol%). The sealed vial was evacuated and flushed

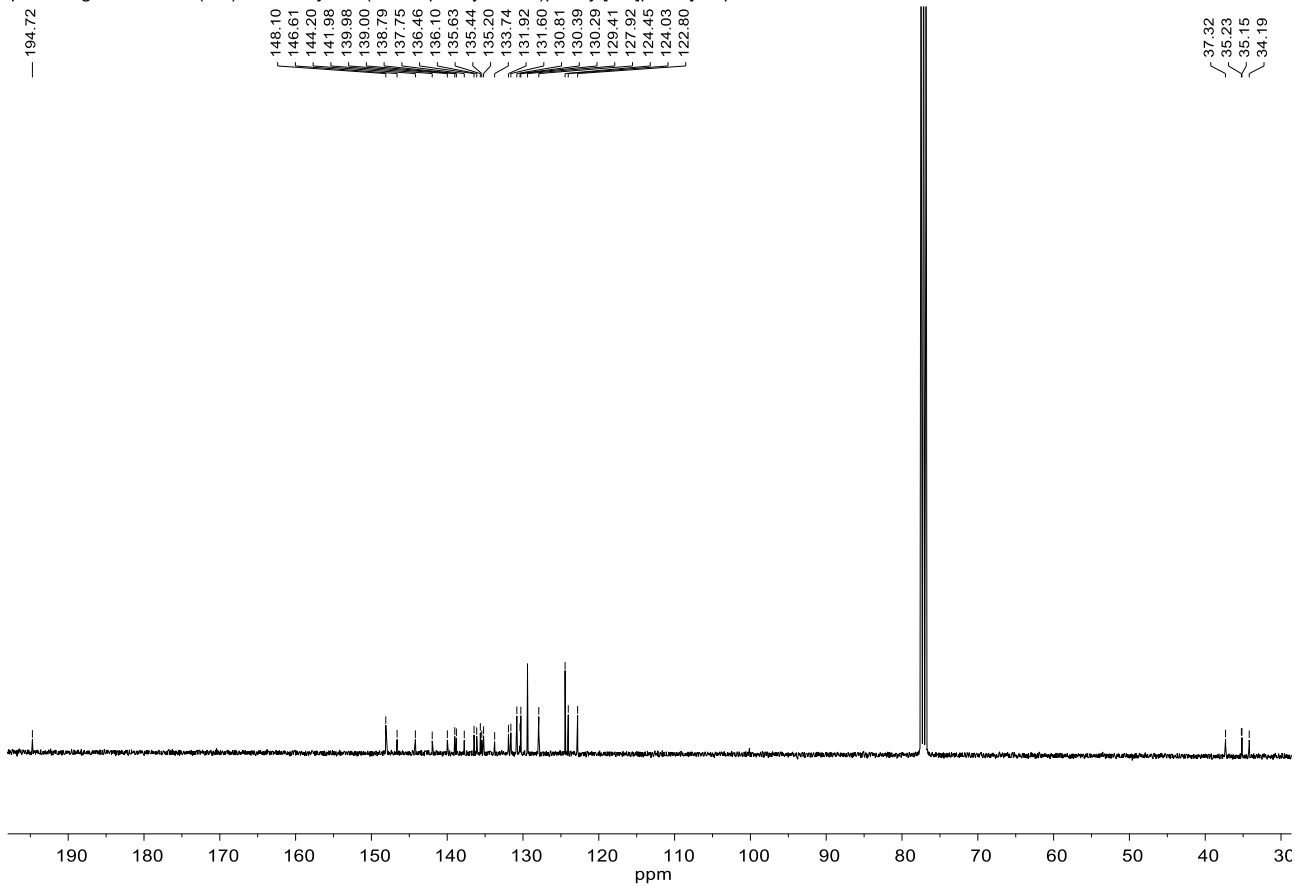
with argon three times. Through the septum 7 mL of degassed toluene and 1 mL of degassed water were added, then heated to 75  $^{\circ}C$  and stirred for 16 h. The reaction mixture was diluted in 50 mL of ethyl acetate and washed first with sat. aqueous  $NH_4Cl$  solution (3  $\times$  30 mL) and then with brine (30 mL). The organic layer was dried over  $Na_2SO_4$  and the solvent was removed under reduced pressure. The crude product was purified by column chromatography (silica gel, gradient of cyclohexane/ethyl acetate; 50/1 to 20/1) to yield 145 mg of the product as an off-white solid (261  $\mu$ mol, 65%).

$R_f = 0.26$  (CH/EA 20:1) = 0.26. –  $^1H$  NMR (400 MHz,  $CDCl_3$ )  $\delta$  = 7.44 (t,  $J$  = 7.3 Hz, 1H), 7.36 – 7.29 (m, 5H), 7.28 – 7.20 (m, 7H), 7.16 – 7.02 (m, 6H), 6.96 (d,  $J$  = 1.9 Hz, 1H), 6.87 (dd,  $J$  = 7.7, 1.8 Hz, 1H), 6.76 (dd,  $J$  = 11.6, 7.7 Hz, 2H), 6.57 (dd,  $J$  = 7.6, 1.9 Hz, 1H), 6.51 (d,  $J$  = 1.9 Hz, 1H), 3.82 (ddd,  $J$  = 13.3, 9.2, 6.6 Hz, 1H), 3.47 – 3.35 (m, 1H), 3.33 – 3.22 (m, 1H), 3.20 – 3.08 (m, 2H), 3.07 – 2.89 (m, 2H), 2.87 – 2.73 (m, 1H) ppm. –  $^{13}C$  NMR (101 MHz,  $CDCl_3$ )  $\delta$  = 194.72 ( $C_{quat.}$ , CO), 148.10 ( $C_{quat.}$ ), 146.61 ( $C_{quat.}$ ), 144.20 ( $C_{quat.}$ ), 141.98 ( $C_{quat.}$ ), 139.98 ( $C_{quat.}$ ), 139.00 ( $C_{quat.}$ ), 138.79 ( $C_{quat.}$ ), 137.75 ( $C_{quat.}$ ), 136.46 (+), 136.10 (+), 135.63 (+), 135.44 ( $C_{quat.}$ ), 135.20 (+), 133.74 ( $C_{quat.}$ ), 131.92 (+), 131.60 (+), 130.81 (+), 130.39 (+), 130.29 (+), 129.41 (+), 127.92 (+), 124.45 (+), 124.03 (+), 122.80 (+), 37.32 (–), 35.23 (–), 35.15 (–), 34.19 (–) ppm. – Mp : 91-95  $^{\circ}C$ . – IR (ATR):  $\tilde{\nu}$  = 2922 (vw), 1736 (w), 1649 (w), 1588 (w), 1509 (w), 1486 (w), 1445 (w), 1316 (w), 1268 (m), 1175 (w), 1074 (vw), 1046 (vw), 977 (vw), 916 (vw), 834 (w), 800 (vw), 751 (w), 696 (m), 661 (w), 648 (w), 634 (w), 550 (vw), 512 (w), 489 (vw)  $cm^{-1}$ . – MS (FAB, 3-NBA),  $m/z$ : 556  $[M+H]^+$ , 555  $[M]^+$ . – HRMS ( $C_{41}H_{33}NO$ ) calc.: 555.2562; found: 555.2561.

pseudo-geminal "cis" (rac)-4-Benzoyl-13-(4'-N-diphenylamino)phenyl[2.2]paracyclophane



pseudo-geminal "cis" (rac)-4-Benzoyl-13-(4'-N-diphenylamino)phenyl[2.2]paracyclophane



S19

### 3. Photophysical Characterization

*Photophysical measurements.* Optically dilute solutions of concentrations in the order of  $10^{-5}$  or  $10^{-6}$  M were prepared in HPLC grade solvent for absorption and emission analysis. Absorption spectra were recorded at room temperature on a Shimadzu UV-1800 double beam spectrophotometer. Aerated solutions were bubbled with compressed air for 5 minutes whereas degassed solutions were prepared via three freeze-pump-thaw cycles prior to emission analysis using an in-house adapted fluorescence cuvette, itself purchased from Starna. Steady-state emission and time-resolved emission spectra were recorded at 298 K using an Edinburgh Instruments F980 fluorimeter. Samples were excited at 360 nm for steady-state measurements and at 378 nm for time-resolved measurements. Photoluminescence quantum yields for solutions were determined using the optically dilute method<sup>8</sup> in which four sample solutions with absorbance at 360 nm being ca. 0.10, 0.080, 0.060 and 0.040 were used. Their emission intensities were compared with those of a reference, quinine sulfate, whose quantum yield ( $\Phi_r$ ) in 1 N H<sub>2</sub>SO<sub>4</sub> was determined to be 54.6% using absolute method.<sup>9</sup> The quantum yield of sample,  $\Phi_{PL}$ , can be determined by the equation  $\Phi_{PL} = \Phi_r(A_r/A_s)((I_s/I_r)(n_s/n_r)^2)$ , where A stands for the absorbance at the excitation wavelength ( $\lambda_{exc}$ : 360 nm), I is the integrated area under the corrected emission curve and n is the refractive index of the solvent with the subscripts “s” and “r” representing sample and reference respectively. An integrating sphere was employed for quantum yield measurements for thin film samples.

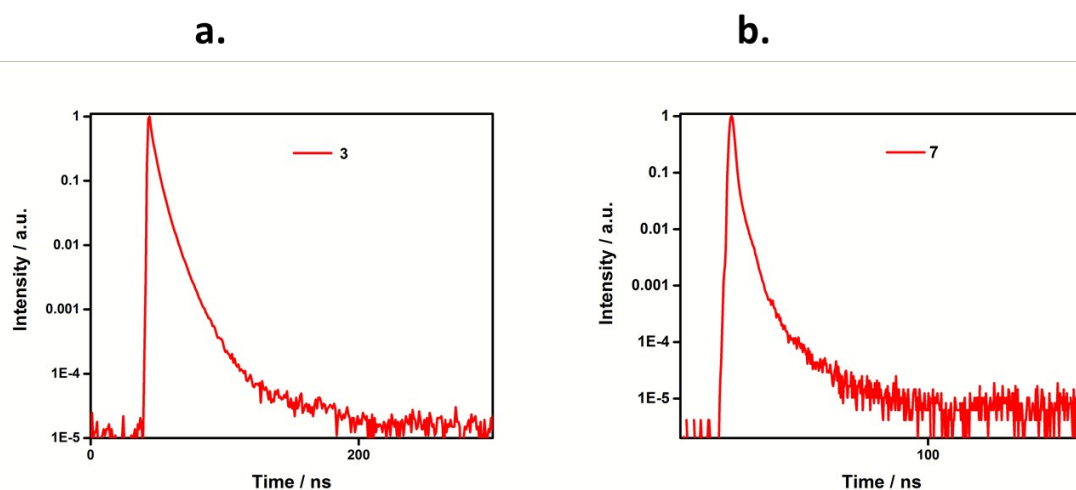


Figure S1. Transient PL decay profiles of a.) **3** and b.) **7** in degassed PhMe ( $\lambda_{exc} = 378$  nm).

### 3.1 Evaluation of lifetimes.

Prompt and delayed lifetimes were determined by a bi-exponential fit of the decay curves using the following parameters:

$$y = ae^{-t/\tau_p} + be^{-t/\tau_d}$$

where, a and b are the pre exponential factors,  $\tau_p$  and  $\tau_d$  are the prompt and delayed components and t, time is the variable parameter.

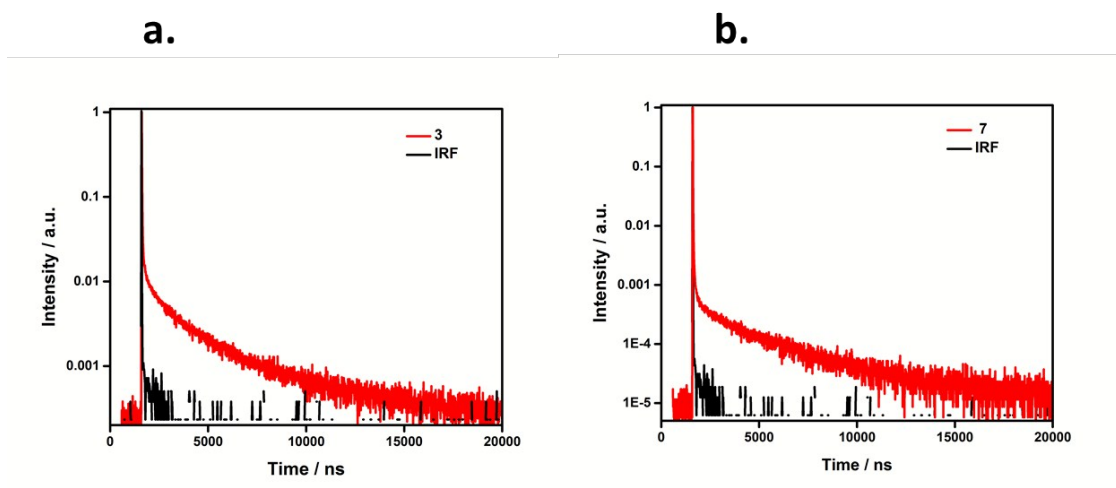


Figure S2. Transient PL decay profiles of a.) **3** and b.) **7** in 15 wt.% doped films in mCP ( $\lambda_{\text{exc}}$  378 nm), where IRF is the instrument response function.

Table S1. Absolute  $\Phi_{\text{PL}}$  measurements of doped films of **3** and **7** in different host materials as a function of doping concentrations.

Host Material <sup>a</sup>	$\Phi_{\text{PL}} / \%$	
	<b>3</b>	<b>7</b>
1 wt. % DPEPO	4.0	3.8
3 wt. % DPEPO	4.2	4.4
5 wt. % DPEPO	5.0	4.5
7 wt. % PPT	7.0	8.3

1 wt. % CzSi	7.7	7.6
3 wt. % CzSi	7.8	8.8
10 wt. % CzSi	8.6	9.3
1 wt. % mCP	7.0	7.0
3 wt. % mCP	7.4	7.7
15 wt. % mCP	12.2	15.0
20 wt. % mCP	5.0	4.3
25 wt.% mCP	2.1	3.6

<sup>a</sup> Thin films were prepared by vacuum deposition and values were determined using an integrating sphere ( $\lambda_{\text{exc}} = 360 \text{ nm}$ ); degassing was done by  $\text{N}_2$  purge.

### 3.2 Evaluation of rate constants.

The absolute rate constants for a radiative and non-radiative processes can only be explicitly calculated for a monoexponential decay. For a bi- or multiexponential decay, we assumed that the  $k_{\text{nr}}^{\text{S}}$  approaches zero and therefore the intersystem crossing can be defined as  $\Phi_{\text{ISC}} = 1 - \Phi_{\text{p}}$ .<sup>14</sup> following the method described by Masui *et al.*<sup>14</sup> The rate constants ( $k_{\text{r}}^{\text{S}}$ ,  $k_{\text{nr}}^{\text{T}}$ ,  $k_{\text{ISC}}$ ,  $k_{\text{rISC}}$ ) associated with **3** and **7** were evaluated as follows, where

$k_{\text{p}}$  and  $k_{\text{d}}$  represent the prompt and delayed fluorescence rates which were calculated from the experimentally measured prompt and delayed lifetimes:

$$k_{\text{p}} = 1 / \tau_{\text{p}}, \quad k_{\text{d}} = 1 / \tau_{\text{d}}.$$

The prompt and delayed fluorescence quantum efficiencies,  $\Phi_{\text{p}}$  and  $\Phi_{\text{d}}$  were determined by integrating the transient PL signal from 0 to 500 ns as the prompt components and from 500 ns to 20  $\mu\text{s}$  as the delayed components.<sup>14</sup>

Therefore,

$$k_{\text{r}}^{\text{S}} = \Phi_{\text{p}} k_{\text{p}}; \quad k_{\text{ISC}} = (1 - \Phi_{\text{p}}) k_{\text{p}}.$$

$$k_{\text{rISC}} = (k_{\text{p}} k_{\text{d}} / k_{\text{ISC}}) * \Phi_{\text{d}} / \Phi_{\text{p}}.$$

$$k_{\text{nr}}^{\text{T}} = k_{\text{d}} - \Phi_{\text{p}} k_{\text{rISC}}$$

where  $k_r^S$  is the radiative decay rate of the singlet state,  $k_{ISC}$  is the intersystem crossing rate,  $k_{rISC}$  is the reverse intersystem crossing rate, and  $k_{nr}^T$  is non-radiative decay rate of the triplet state.

Table S2. Rate constants of isomers **3** and **7**, determined in PhMe and 15 wt.% doped films in mCP.

Material	$k_r^S$ <sup>a</sup> / x 10 <sup>6</sup> s <sup>-1</sup>	$k_r^S$ <sup>b</sup> / x 10 <sup>6</sup> s <sup>-1</sup>	$k_{rISC}$ <sup>a</sup> / x 10 <sup>5</sup> s <sup>-1</sup>	$k_{ISC}$ <sup>b</sup> / x 10 <sup>7</sup> s <sup>-1</sup>	$k_{ISC}$ <sup>a</sup> / x 10 <sup>7</sup> s <sup>-1</sup>	$k_{nr}^T$ <sup>a</sup> / x 10 <sup>5</sup> s <sup>-1</sup>
<b>3</b>	6.3	63	7.0	5.2	71	4.7
<b>7</b>	18	174	3.1	11.0	11	2.4

<sup>a</sup>Calculated from the transient PL spectra measured in 15 wt.% doped films in mCP. <sup>b</sup>Calculated from the transient PL spectra measured in degassed PhMe solution.

#### 4. DFT modelling.

##### Computational methodology

The calculations were performed with the Gaussian 09<sup>10</sup> revision D.018 suite. Initially the geometries of all the derivatives were fully optimized using a DFT methodology employing the PBE0<sup>11</sup> functional with the standard Pople<sup>12</sup> 6-31G(d,p) basis set and Tamm–Dancoff approximation (TDA) was treated as a variant of Time-dependent density functional theory (TD-DFT). The molecular orbitals were visualized using GaussView 5.0 software<sup>13</sup>.

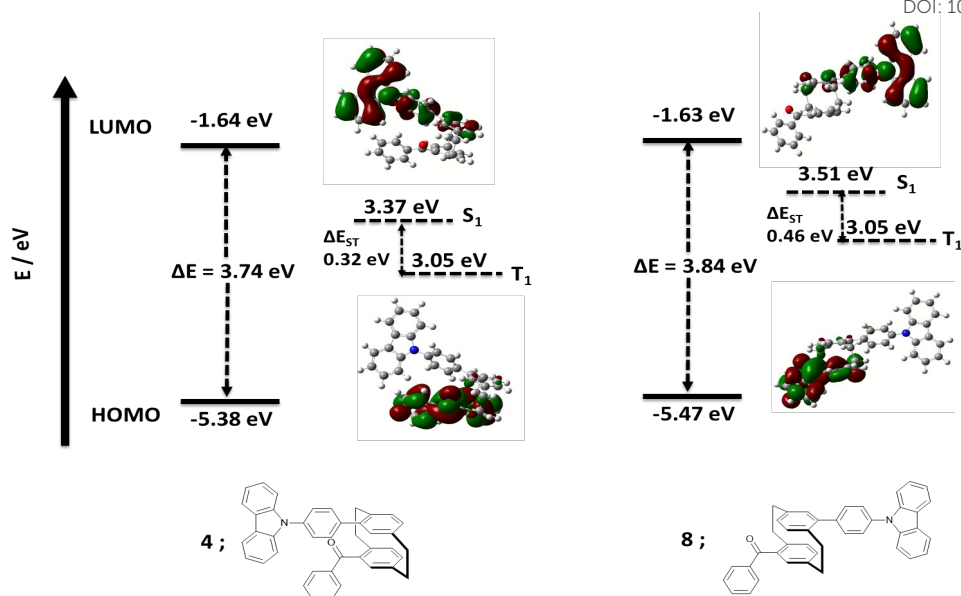


Figure S3. HOMO-LUMO profiles and excited state dynamics of cis and trans isomers **4** and **8**, respectively (PBE0/6-31G(d,p)).

Table S3. Optimized atomic coordinates of isomer **3** obtained from DFT calculations.

-----						
Center	Atomic	Atomic	Coordinates (Angstroms)			
Number	Number	Type	X	Y	Z	
-----						
1	6	0	1.933515	-1.932747	0.211264	
2	6	0	2.754054	-2.283639	1.305525	
3	6	0	4.031951	-2.772284	1.015989	
4	6	0	4.606983	-2.638072	-0.240321	
5	6	0	3.898334	-1.995732	-1.256698	
6	6	0	2.535774	-1.798333	-1.049342	
7	1	0	5.653281	-2.897477	-0.383184	
8	1	0	1.951976	-1.355286	-1.850336	

9	6	0	4.596044	-1.280430	-2.383054
10	1	0	3.888438	-1.101920	-3.194878
11	1	0	5.421765	-1.881722	-2.778185
12	6	0	2.455727	-1.942875	2.743274
13	6	0	5.183350	0.126740	-1.938155
14	1	0	4.910269	0.855868	-2.703164
15	1	0	6.275640	0.055945	-1.911511
16	6	0	2.873261	-0.452653	3.128129
17	1	0	1.978040	0.111919	3.410601
18	1	0	3.503982	-0.496754	4.021666
19	6	0	4.713635	0.545715	-0.570025
20	6	0	5.509555	0.227322	0.532520
21	6	0	3.423736	1.043487	-0.290417
22	6	0	4.962823	0.066511	1.800231
23	1	0	6.544260	-0.060721	0.364232
24	6	0	2.891262	0.899397	0.997373
25	6	0	3.596014	0.253655	2.011517
26	1	0	5.579585	-0.343077	2.596866
27	1	0	1.847181	1.154813	1.151404
28	6	0	2.511946	1.500431	-1.371354
29	8	0	2.561132	1.028693	-2.500480
30	6	0	1.487406	2.544771	-1.063668
31	6	0	1.681834	3.532153	-0.093136

32	6	0	0.323762	2.561320	-1.839562
33	6	0	0.724780	4.523827	0.095696
34	1	0	2.592091	3.532360	0.498109
35	6	0	-0.638114	3.542066	-1.639500
36	1	0	0.199605	1.793859	-2.596678
37	6	0	-0.434853	4.528498	-0.674141
38	1	0	0.887459	5.297410	0.840051
39	1	0	-1.545344	3.544291	-2.236414
40	1	0	-1.177933	5.307982	-0.530279
41	1	0	3.024169	-2.623315	3.384473
42	1	0	1.400291	-2.090254	2.987970
43	1	0	4.641692	-3.141482	1.837742
44	6	0	0.492974	-1.595374	0.292553
45	6	0	-0.356923	-2.047110	-0.729706
46	6	0	-0.090434	-0.800436	1.287743
47	6	0	-1.698235	-1.705355	-0.777573
48	1	0	0.054022	-2.680043	-1.510601
49	6	0	-1.437396	-0.469281	1.264657
50	1	0	0.512120	-0.406142	2.094485
51	6	0	-2.261020	-0.902854	0.222017
52	1	0	-2.321113	-2.061717	-1.591437
53	1	0	-1.853279	0.151882	2.050992
54	7	0	-3.618696	-0.535739	0.174984

55	6	0	-4.578787	-1.444679	-0.319634
56	6	0	-4.023574	0.746209	0.602151
57	6	0	-5.592978	-1.004519	-1.177006
58	6	0	-4.526677	-2.795578	0.040783
59	6	0	-5.227927	0.909676	1.296551
60	6	0	-3.228919	1.868764	0.340735
61	6	0	-6.540304	-1.900852	-1.655461
62	1	0	-5.630869	0.042582	-1.459721
63	6	0	-5.467131	-3.687826	-0.458902
64	1	0	-3.742707	-3.135976	0.709718
65	6	0	-5.630485	2.173289	1.710092
66	1	0	-5.842445	0.040037	1.505386
67	6	0	-3.631048	3.123650	0.778868
68	1	0	-2.293395	1.753011	-0.196996
69	6	0	-6.481679	-3.247415	-1.305040
70	1	0	-7.321992	-1.544627	-2.320121
71	1	0	-5.413178	-4.733872	-0.171577
72	1	0	-6.568295	2.282612	2.247098
73	6	0	-4.834360	3.288060	1.460264
74	1	0	-2.994638	3.979507	0.574803
75	1	0	-7.218880	-3.946345	-1.687467
76	1	0	-5.147244	4.272299	1.794507

Table S4. Optimized atomic coordinates of isomer 4 obtained from DFT calculations.

Center Number	Atomic Number	Atomic Type	Coordinates (Angstroms)		
			X	Y	Z
1	6	0	2.035728	-1.918506	-0.100288
2	6	0	2.851830	-2.426739	0.932614
3	6	0	4.142091	-2.835980	0.580587
4	6	0	4.721832	-2.484955	-0.630264
5	6	0	4.008980	-1.699514	-1.537207
6	6	0	2.639575	-1.569905	-1.317912
7	1	0	5.774638	-2.695916	-0.802052
8	1	0	2.048364	-1.021193	-2.045044
9	6	0	4.707039	-0.800936	-2.522750
10	1	0	4.005077	-0.497144	-3.301266
11	1	0	5.541923	-1.322250	-3.003049
12	6	0	2.534074	-2.331320	2.402832
13	6	0	5.277253	0.517036	-1.844733
14	1	0	4.996757	1.360939	-2.477576
15	1	0	6.370301	0.455692	-1.826694
16	6	0	2.950772	-0.929355	3.038141
17	1	0	2.053284	-0.422902	3.409628
18	1	0	3.577820	-1.124915	3.913704
19	6	0	4.799173	0.696283	-0.427820
20	6	0	5.594988	0.209564	0.611787
21	6	0	3.499422	1.119435	-0.077758
22	6	0	5.045546	-0.171582	1.830907
23	1	0	6.635132	-0.029946	0.405124
24	6	0	2.967859	0.758195	1.165997

## ChemComm

25	6	0	3.675616	-0.040489	2.062080
26	1	0	5.665071	-0.702110	2.550266
27	1	0	1.922911	0.980224	1.357436
28	6	0	2.576168	1.724187	-1.074177
29	8	0	2.643243	1.447620	-2.265229
30	6	0	1.509810	2.656892	-0.599718
31	6	0	1.675826	3.491443	0.509946
32	6	0	0.326488	2.723523	-1.341960
33	6	0	0.668696	4.380192	0.871035
34	1	0	2.600607	3.452840	1.077137
35	6	0	-0.684988	3.598743	-0.970640
36	1	0	0.222089	2.075678	-2.206201
37	6	0	-0.512642	4.430166	0.135832
38	1	0	0.807166	5.036413	1.724950
39	1	0	-1.611693	3.630978	-1.535263
40	1	0	-1.299338	5.123039	0.420754
41	1	0	3.090082	-3.113347	2.928489
42	1	0	1.474700	-2.512038	2.603782
43	1	0	4.754202	-3.322537	1.336710
44	6	0	0.586660	-1.627404	0.022513
45	6	0	-0.253543	-1.981145	-1.045017
46	6	0	-0.001303	-0.965029	1.107634
47	6	0	-1.603903	-1.665949	-1.047341
48	1	0	0.172428	-2.508829	-1.892947
49	6	0	-1.356103	-0.660790	1.124928
50	1	0	0.601456	-0.657659	1.951156
51	6	0	-2.165121	-0.997451	0.041701
52	1	0	-2.229352	-1.923847	-1.896151
53	1	0	-1.793213	-0.152796	1.978548

54	7	0	-3.530829	-0.649926	0.042780
55	6	0	-4.034011	0.629881	0.249276
56	6	0	-4.594591	-1.515840	-0.182649
57	6	0	-3.347485	1.820849	0.477022
58	6	0	-5.444274	0.588492	0.154361
59	6	0	-4.582150	-2.892332	-0.400137
60	6	0	-5.802781	-0.783120	-0.119389
61	6	0	-4.103146	2.976381	0.627863
62	1	0	-2.264531	1.850752	0.523025
63	6	0	-6.178047	1.765475	0.310905
64	6	0	-5.805857	-3.525593	-0.574832
65	1	0	-3.651524	-3.449220	-0.423944
66	6	0	-7.018176	-1.445108	-0.298777
67	6	0	-5.502848	2.954098	0.551034
68	1	0	-3.592127	3.917328	0.810471
69	1	0	-7.261891	1.749550	0.240802
70	6	0	-7.012640	-2.813515	-0.529768
71	1	0	-5.825335	-4.597682	-0.746539
72	1	0	-7.954116	-0.895699	-0.252811
73	1	0	-6.061294	3.876448	0.676706
74	1	0	-7.950620	-3.340999	-0.671920

Table S5. Optimized atomic coordinates of isomer **6** obtained from DFT calculations.

Center Number	Atomic Number	Atomic Type	Coordinates (Angstroms)		
			X	Y	Z
1	6	0	-0.608969	-1.578992	-0.253143
2	6	0	-1.414522	-1.287815	-1.376353

3	6	0	-2.677019	-1.880442	-1.426694
4	6	0	-3.247392	-2.484423	-0.312129
5	6	0	-2.563353	-2.487174	0.903535
6	6	0	-1.205280	-2.164887	0.867347
7	1	0	-3.289820	-1.730907	-2.312976
8	1	0	-4.285156	-2.801935	-0.341254
9	1	0	-0.610047	-2.277733	1.770971
10	6	0	-3.316702	-2.573598	2.204852
11	1	0	-2.731761	-3.112108	2.957907
12	1	0	-4.248406	-3.120619	2.048079
13	6	0	-1.131963	-0.138220	-2.317808
14	1	0	-1.836250	-0.208639	-3.152619
15	6	0	-3.689115	-1.147283	2.800101
16	1	0	-4.750397	-1.162915	3.054237
17	6	0	-1.308342	1.276033	-1.630028
18	1	0	-0.317133	1.666841	-1.380349
19	1	0	-1.745295	1.957475	-2.368320
20	6	0	-3.355132	-0.024786	1.855487
21	6	0	-4.111997	0.288909	0.706593
22	6	0	-2.116907	0.608149	1.973066
23	6	0	-3.488467	0.899911	-0.388541
24	6	0	-1.508706	1.213781	0.879809
25	6	0	-2.130318	1.212375	-0.369900

26	1	0	-4.045987	0.988966	-1.317738
27	1	0	-0.481466	1.558738	0.962701
28	1	0	-3.121774	-0.995139	3.724025
29	1	0	-1.553016	0.488961	2.895573
30	6	0	-5.510689	-0.191355	0.553319
31	8	0	-5.870689	-1.276822	0.992365
32	6	0	-6.494282	0.676499	-0.161756
33	6	0	-6.342595	2.062566	-0.274842
34	6	0	-7.640455	0.066207	-0.682720
35	6	0	-7.317667	2.821846	-0.913015
36	1	0	-5.469497	2.545374	0.151822
37	6	0	-8.605366	0.823324	-1.330904
38	1	0	-7.749132	-1.006849	-0.561581
39	6	0	-8.444296	2.203575	-1.447679
40	1	0	-7.199281	3.898476	-0.989573
41	1	0	-9.487121	0.341905	-1.743142
42	1	0	-9.201607	2.797637	-1.951006
43	6	0	0.806366	-1.156843	-0.186662
44	6	0	1.343355	-0.568831	0.965858
45	6	0	1.664625	-1.358344	-1.276149
46	6	0	2.674900	-0.180094	1.025079
47	1	0	0.703717	-0.411432	1.828254
48	6	0	2.990265	-0.951450	-1.237180

49	1	0	1.281311	-1.851303	-2.164416
50	6	0	3.503143	-0.354459	-0.083906
51	1	0	3.083586	0.259316	1.929521
52	1	0	3.636379	-1.088970	-2.098371
53	7	0	4.845677	0.071507	-0.039524
54	6	0	5.957767	-0.706412	-0.343843
55	6	0	5.275565	1.351118	0.295948
56	6	0	6.024807	-2.052670	-0.697541
57	6	0	7.121860	0.083481	-0.200057
58	6	0	4.524899	2.475512	0.634055
59	6	0	6.686045	1.398198	0.207551
60	6	0	7.282920	-2.593988	-0.928632
61	1	0	5.128405	-2.657772	-0.780810
62	6	0	8.373319	-0.486104	-0.438249
63	6	0	5.214019	3.650287	0.906463
64	1	0	3.441646	2.436614	0.675788
65	6	0	7.353096	2.591741	0.486730
66	6	0	8.446725	-1.822153	-0.806157
67	1	0	7.363707	-3.640546	-1.206833
68	1	0	9.275875	0.108856	-0.332055
69	6	0	6.612818	3.711391	0.839465
70	1	0	4.653430	4.541054	1.174025
71	1	0	8.436286	2.642266	0.423460

72	1	0	9.413423	-2.277823	-0.996101
73	1	0	7.118852	4.645767	1.061027
74	1	0	-0.129460	-0.167013	-2.750698

Table S6. Optimized atomic coordinates of isomer **7** obtained from DFT calculations.

-----					
Center	Atomic	Atomic	Coordinates (Angstroms)		
Number	Number	Type	X	Y	Z
-----					
1	6	0	-0.402561	-1.483722	0.016601
2	6	0	-1.207633	-1.483018	-1.143303
3	6	0	-2.460267	-2.092891	-1.054847
4	6	0	-3.022922	-2.419949	0.171937
5	6	0	-2.337434	-2.139129	1.356427
6	6	0	-0.986432	-1.813823	1.245428
7	1	0	-3.071859	-2.169308	-1.951585
8	1	0	-4.056622	-2.750336	0.221357
9	1	0	-0.387918	-1.702535	2.147255
10	6	0	-3.102059	-1.932928	2.637224
11	1	0	-2.523678	-2.272171	3.503233
12	1	0	-4.029671	-2.507245	2.602879
13	6	0	-0.917234	-0.591138	-2.328028
14	1	0	0.140534	-0.324801	-2.347598

15	1	0	-1.130103	-1.112700	-3.267443
16	6	0	-3.488855	-0.412837	2.870511
17	1	0	-4.510128	-0.385827	3.255751
18	6	0	-1.767901	0.750576	-2.314198
19	1	0	-1.104906	1.572189	-2.606115
20	1	0	-2.546747	0.684458	-3.080519
21	6	0	-3.328081	0.412999	1.621662
22	6	0	-4.220983	0.392120	0.532324
23	6	0	-2.109484	1.063918	1.413494
24	6	0	-3.748966	0.697096	-0.751863
25	6	0	-1.648724	1.357008	0.136900
26	6	0	-2.413434	1.020316	-0.981960
27	1	0	-4.407137	0.523895	-1.599963
28	1	0	-0.626649	1.704996	0.007457
29	1	0	-2.826367	0.002523	3.637089
30	1	0	-1.440189	1.198438	2.260017
31	6	0	-5.592842	-0.162658	0.669904
32	8	0	-5.829663	-1.117215	1.400251
33	6	0	-6.701149	0.459100	-0.115514
34	6	0	-6.646841	1.773599	-0.590665
35	6	0	-7.856885	-0.300618	-0.325677
36	6	0	-7.729523	2.312995	-1.277289
37	1	0	-5.762551	2.375347	-0.407833

38	6	0	-8.930461	0.234356	-1.022676
39	1	0	-7.885008	-1.309937	0.072344
40	6	0	-8.867448	1.543072	-1.500344
41	1	0	-7.685756	3.336926	-1.636031
42	1	0	-9.820455	-0.364206	-1.192649
43	1	0	-9.709468	1.963966	-2.042275
44	6	0	1.003877	-1.029895	-0.007186
45	6	0	1.499187	-0.129669	0.944171
46	6	0	1.901508	-1.511696	-0.969668
47	6	0	2.827027	0.272682	0.940911
48	1	0	0.827994	0.261655	1.703025
49	6	0	3.225622	-1.102237	-0.995526
50	1	0	1.547940	-2.227046	-1.706889
51	6	0	3.707758	-0.204229	-0.035699
52	1	0	3.190210	0.966962	1.691886
53	1	0	3.902385	-1.485435	-1.752479
54	7	0	5.055344	0.206837	-0.051743
55	6	0	6.072480	-0.728921	-0.334405
56	6	0	5.995494	-2.032113	0.169999
57	6	0	7.170351	-0.365744	-1.122817
58	6	0	6.995141	-2.952499	-0.118399
59	1	0	5.147137	-2.314477	0.785006
60	6	0	8.174124	-1.288359	-1.388829

61	1	0	7.228870	0.642722	-1.519386
62	6	0	8.092576	-2.587526	-0.893962
63	1	0	6.920703	-3.960087	0.280227
64	1	0	9.020285	-0.991094	-2.001513
65	1	0	8.875338	-3.307552	-1.110698
66	6	0	5.387663	1.545108	0.242524
67	6	0	6.513563	1.843325	1.018591
68	6	0	4.593255	2.593034	-0.237095
69	6	0	6.839107	3.164600	1.297881
70	1	0	7.127797	1.032663	1.396858
71	6	0	4.916778	3.909739	0.064638
72	1	0	3.723089	2.363876	-0.843819
73	6	0	6.042641	4.206071	0.828860
74	1	0	7.716345	3.379180	1.901332
75	1	0	4.289913	4.711452	-0.314962
76	1	0	6.296351	5.236667	1.056016

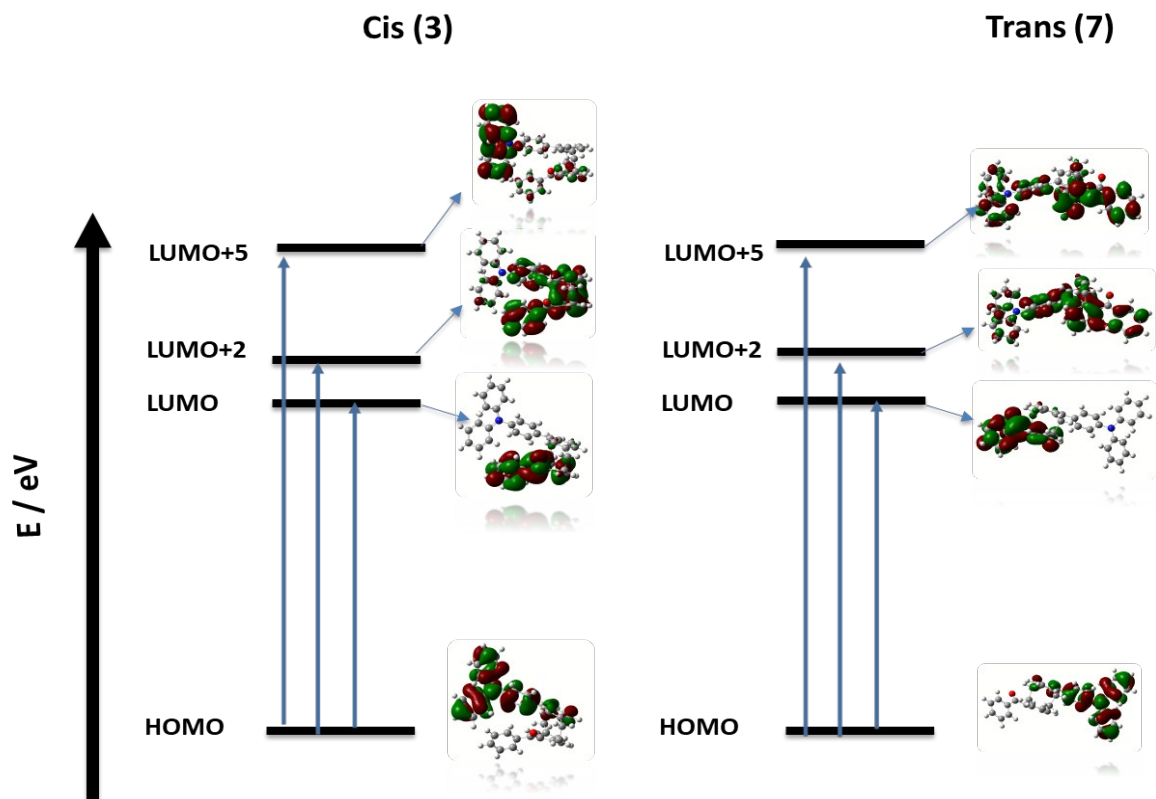


Figure S4. Natural transition orbital diagrams for the transitions H  $\rightarrow$  L, H  $\rightarrow$  L+2 and H  $\rightarrow$  L+5 in isomers **3** and **7**.

## 5. References

1. Phane Nomenclature - Part I: Phane Parent Names, <http://www.chem.qmul.ac.uk/iupac/phane/>, (accessed 07/May/2018).
2. F. Vögtle and P. Neumann, *Tetrahedron Lett.*, 1969, **60**, 5329–5334.
3. R. S. Cahn, C. Ingold and V. Prelog, *Angew. Chem. Int. Ed.*, 1966, **5**, 385–415.
4. W. C. Still, M. Kahn and A. Mitra, *J. Org. Chem.*, 1978, **43**, 2923–2925.
5. H. J. Reich and D. J. Cram, *J. Am. Chem. Soc.*, 1969, **91**, 3527–3533.

6. C. Braun, E. Spuling, N. B. Heine, M. Cakici, M. Nieger and S. Bräse, *Adv. Synth. Catal.*, 2016, **358**, 1664-1670.
7. A. Izuoka, S. Murata, T. Sugawara and H. Iwamura, *J. Am. Chem. Soc.*, 1987, **109**, 2631–2639.
8. J. N. Demas and G. A. Crosby, *J. Phys. Chem.*, 1971, **75**, 991-1024.
9. W. H. Melhuish, *J. Phys. Chem.*, 1961, **65**, 229-235.
10. M. J. Frisch, G. W. Trucks, H. B. Schlegel, G. E. Scuseria, M. A. Robb, J. R. Cheeseman, G. Scalmani, V. Barone, B. Mennucci, G. A. Petersson, H. Nakatsuji, M. Caricato, X. Li, H. P. Hratchian, A. F. Izmaylov, J. Bloino, G. Zheng, J. L. Sonnenberg, M. Hada, M. Ehara, K. Toyota, R. Fukuda, J. Hasegawa, M. Ishida, T. Nakajima, Y. Honda, O. Kitao, H. Nakai, T. Vreven, J. A. Montgomery, Jr., J. E. Peralta, F. Ogliaro, M. Bearpark, J. J. Heyd, E. Brothers, K. N. Kudin, V. N. Staroverov, T. Keith, R. Kobayashi, J. Normand, K. Raghavachari, A. Rendell, J. C. Burant, S. S. Iyengar, J. Tomasi, M. Cossi, N. Rega, J. M. Millam, M. Klene, J. E. Knox, J. B. Cross, V. Bakken, C. Adamo, J. Jaramillo, R. Gomperts, R. E. Stratmann, O. Yazyev, A. J. Austin, R. Cammi, C. Pomelli, J. W. Ochterski, R. L. Martin, K. Morokuma, V. G. Zakrzewski, G. A. Voth, P. Salvador, J. J. Dannenberg, S. Dapprich, A. D. Daniels, O. Farkas, J. B. Foresman, J. V. Ortiz, J. Cioslowski, and D. J. Fox, *Gaussian 09*, Revision D.01. Wallingford, CT, 2013.
11. C. Adamo and V. Barone, *J. Chem. Phys.*, 1999, **110**, 6.
12. A. J. Pople, J. S. Binkley and R. Seeger, *Int. J. Quant. Chem. Symp.*, 1976, **10**, 1.
13. M. Moral, L. Muccioli, W. J. Son, Y. Olivier and J. C. Sancho-García, *J. Chem. Theory Comput.*, 2015, **11**, 168.
14. K. Masui, H. Nakanotani and C. Adachi, *Org. Electron.*, 2013, **14**, 2721.